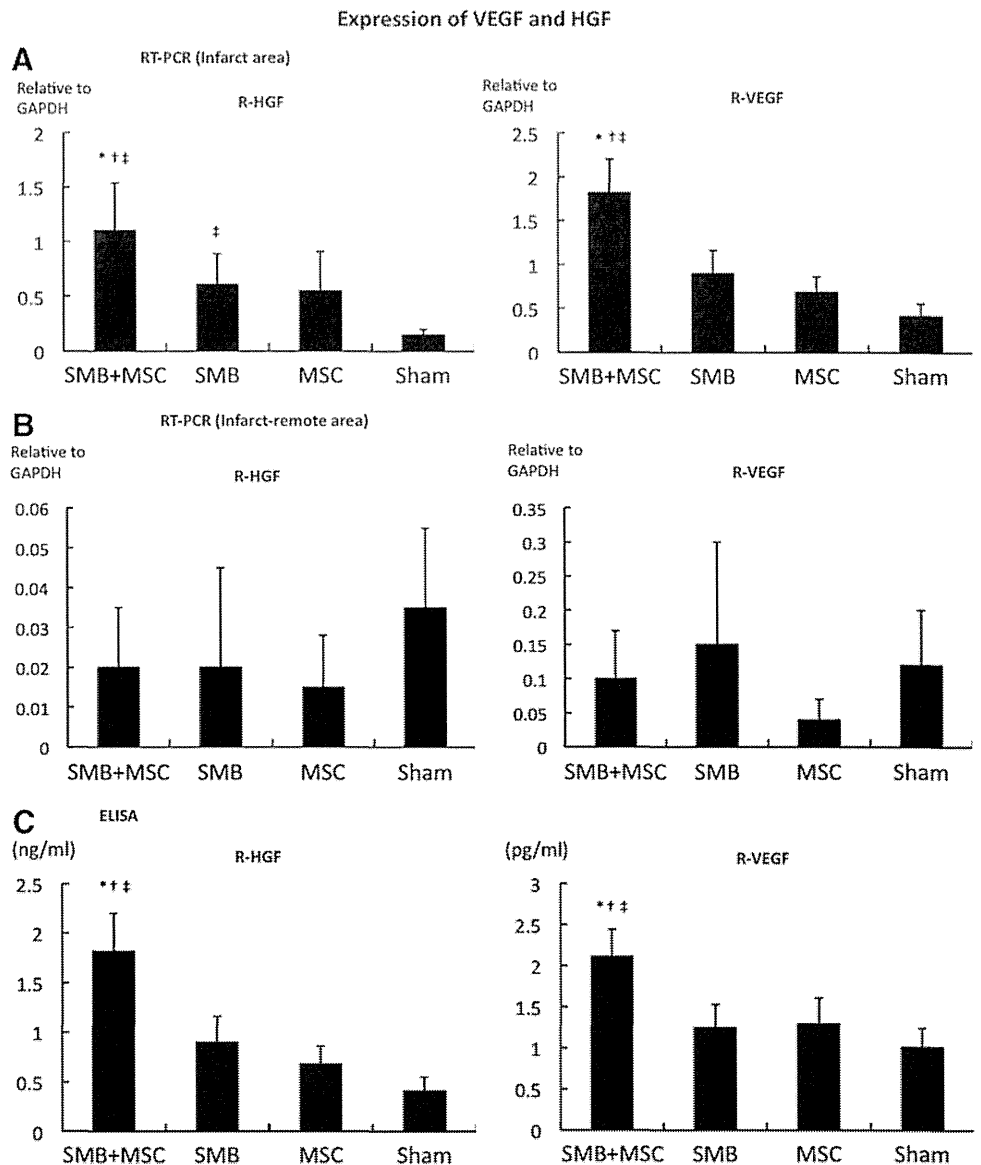


**FIG. 6.** Cell survival. **(A)** Survival of transplanted cells of rat origin was significantly greater in the SMB+MSC sheet group than in the SMB sheet group.  $N = 4$  in each group.  $*p < 0.05$ . **(B)** The number of terminal deoxynucleotidyl transferase-mediated dUTP nick end labeling (TUNEL)-positive myocytes was significantly lower in SMB+MSC group than in control.  $N = 4$  in each group.  $*p < 0.05$ . **(C)** Expressions of mRNA in the transplanted infarct area of hearts were determined by real-time PCR using rat-specific primers. The expressions of Akt-1 and Bcl<sub>2</sub> mRNA were significantly increased in the SMB+MSC sheet group compared with the other groups.  $N = 4$  in each group.  $*p < 0.05$ . **(D)** Western blotting showed that Bcl<sub>2</sub> was much more enhanced, and cleaved PARP was significantly downregulated in the SMB+MSC group. There was no significant difference in the ratio of phosphorylation of Akt over Akt.  $N = 3$  in each group.  $*p < 0.05$  versus SMB.  $†p < 0.05$  versus MSC.  $‡p < 0.05$  versus control. Error bars = SD. Color images available online at [www.liebertpub.com/tea](http://www.liebertpub.com/tea)

sheets' release of HGF and VEGF but not of IGF-1, bFGF, or SDF-1, *in vitro*. The transplantation of SMB-only cell sheets into the chronically ischemic failing rat heart resulted in reversed LV remodeling, including increased capillaries, attenuated collagen accumulation, and prolonged cell survival, which increased global functional recovery, mediated by the paracrine effects of upregulated HGF and VEGF in the myocardium.

Recent studies, including ours,<sup>3-9</sup> have suggested that a paracrine effect mediated by cytokines secreted from the transplanted cell sheets is a likely mechanism for the therapeutic effects on the myocardium, which was a focus of the present study. Here, we added h-MSCs to the cell sheets to enhance the potential performance of the transplanted r-SMB sheets. Our *in vitro* findings, that h-MSCs enhanced rat mRNA levels and the secretion of cytokines such as r-HGF

**FIG. 7.** Expression of VEGF and HGF is higher at the infarct area. **(A, B)** Levels of mRNA in the transplanted infarct and infarct-remote heart areas by real-time PCR using rat-specific primers. The HGF and VEGF mRNA expressions within the transplanted infarct area of the hearts were significantly increased in the SMB+MSC sheet group compared with the other groups.  $N=4$  in each group.  $*p < 0.05$  versus SMB.  $†p < 0.05$  versus MSC.  $‡p < 0.05$  versus sham. **(C)** Intramyocardial protein levels of HGF and VEGF, analyzed by ELISA, were significantly greater in the heart in the SMB+MSC sheet group compared with the other groups.  $*p < 0.05$  versus SMB.  $†p < 0.05$  versus MSC.  $‡p < 0.05$  versus control. Error bars = SD.



and r-VEGF from r-SMBs, suggested that transplanted cultured cell sheets would secrete r-HGF and r-VEGF *in vivo*. Although the exact mechanisms by which “feeder layers” support cell growth have not been elucidated, it is possible that h-MSCs enhance the r-SMBs directly (via cellular interaction) or indirectly (via secreted cytokines from the h-MSCs).<sup>16</sup> A more comprehensive examination aimed at differentiating these effects might help reveal how feeder layers work.

HGF and VEGF participate in many complex molecular and cellular mechanisms, and their signaling pathways have been intensively investigated *in vivo*.<sup>3,9</sup> SMBs or MSCs act as the natural supplier of both HGF and VEGF and provide feasible and safe sources for cell therapy in clinical applications. Indeed, SMBs and bone marrow-derived mesenchymal stem cell sheets can secrete growth factors (e.g., HGF and VEGF) into the myocardium and accelerate neovascularization in the damaged area.<sup>5-8</sup> More recent reports have revealed that angiogenesis induced by HGF or VEGF, an

antifibrotic effect promoted by HGF, or the migration and survival of SMBs supported by VEGF,<sup>17</sup> could be beneficial to an impaired heart.<sup>7,8</sup> In addition, our data from a cytokine/chemokine multiplex immunology assay indicate that leptin may also be beneficial (e.g., by inducing angiogenesis through the Jak/STAT pathway).<sup>18</sup> Other cytokines may also contribute to the improvement of cardiac function by single-cell-type cell sheets in as-yet-undiscovered ways.

The mechanism by which the implanted cell sheet attenuates ventricular remodeling and improves cardiac function seems to depend on the cell sheet being placed over the scarred area of the myocardium and leads to repair of the anterior wall thickness, reduction of LV wall stress, and the improvement of ejection performance.<sup>3</sup> Previous studies indicated that the surviving myocardium and implanted cell sheet attenuate complex cellular and molecular events, including hypertrophy, fibrosis, apoptosis of the myocardium, and the pathological accumulation of extracellular matrix.<sup>9</sup> Similarly, the greater cellularity observed after cell-sheet

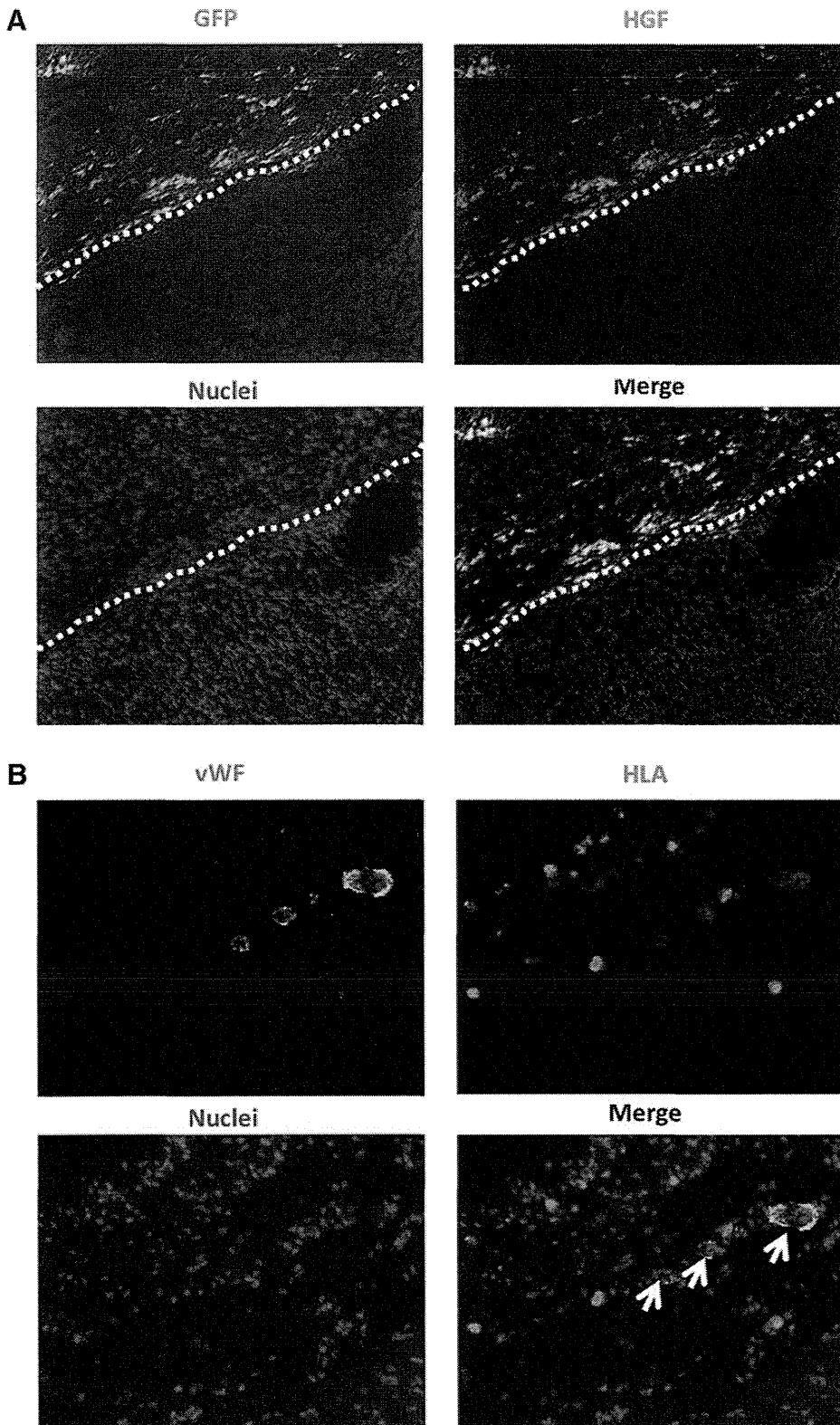


**FIG. 8.** Characterization of transplanted cells. **(A)** Cryosections were stained with an antibody to HGF to detect the distribution of SMB and HGF in the heart. HGF expressions and GFP-positive cells were found in the myocardium after transplantation of the SMB+MSC sheet. White broken line shows the border between the transplanted cell sheet and the host heart. Green indicates GFP; red, HGF; blue, nuclei. **(B)** Cryosections were stained with antibodies to human leukocyte antigen (HLA) and to von Willibrand factor (vWF). Human vWF-positive (white arrows) staining was observed in the host vessels in the h-MSC-transplanted group. Green indicates vWF; red, HLA; blue, nuclei. Color images available online at [www.liebertpub.com/tea](http://www.liebertpub.com/tea)

treatment might have resulted from released SDF-1, which is related to cell migration, adhesion, and proliferation, by the transplanted cell sheet<sup>19,20</sup>

In this study, we performed additional investigations on the paracrine mechanism from a new perspective, by analyzing signaling pathways within the myocardium following

cell-sheet transplantation because the signals induced by released paracrine mediators presumably activate phosphorylation cascades of signaling molecules. We found that STAT3 and Akt phosphorylations were significantly increased, and cleaved PARP was significantly downregulated, 24 h after the co-cultured cell-sheet implantation. Together

with our findings that vascular density was significantly enhanced, and myocardial apoptosis and fibrosis was significantly attenuated in the co-cultured group, it is possible that the co-cultured cell-sheet transplantation induced angiogenesis partially through the Jak/STAT signaling pathway<sup>18</sup> and that it prolonged cell survival by preventing apoptosis through PI-3K/Akt-mediated signaling, which is partially modulated by HGF.<sup>21</sup>

Although we emphasized combining SMBs with h-MSCs, some investigators have focused on different combinations of various cell sources. Sekine *et al.*<sup>22</sup> reported that cardiomyocytes co-cultured with endothelial cells induce greater numbers of capillaries, due to increased secretion of angiogenic growth factors.<sup>22</sup> Another report showed that a dermal fibroblast sheet co-cultured with endothelial progenitor cells was more effective than either single cell-type sheet for improving damaged heart function, accompanied by the inhibition of fibrotic tissue formation and the acceleration of neovascularization in the infarcted myocardium.<sup>23</sup> Thus, the paracrine effect may be improved by combining different cell sources; however, further investigation focused on determining the optimal combinations of cell sources is needed.

Regarding h-MSCs as a cell source, bone marrow-derived or adipose tissue-derived stem cells are reported to differentiate into mature endothelial cells and participate in blood vessel formation in the recipient heart.<sup>24</sup> The presence of endothelial capillary networks improves the survival and organization of implanted cells by maintaining a minimum intercapillary distance to provide oxygen and nutrients. Therefore, the presence of endothelial capillary networks may be partially correlated with cardiac function.

For future tissue engineering for cardiac therapy, the creation of thick cell-dense constructs with functional vessels may be essential. Capillary formation occurs via two basic vessel-constructing processes: angiogenesis, that is, the formation of new capillaries via sprouting or intussusception from pre-existing vessels, and vasculogenesis, which occurs in the developing embryo.<sup>25</sup> Here, the morphology of the vessel formation within myocardial tissues, including the diameter, composition, and fragility of vessel walls, suggested that improper vascularization may occur under pathological conditions. It is likely that not only biological factors but also physical stimuli such as flow and shear stress are required to mimic the *in vivo* environment and enable the formation of mature vascular networks.

A potential limitation of this study is that the exact number of transplanted cells was different in each group *in vivo*. Clinically, open-chest surgery is unlikely to gain easy acceptance except in certain situations; however, less invasive methods (e.g., intracoronary catheter-based procedures) might be technically difficult for carefully placing the cell sheets. Additionally, further studies that include longer timeframe than 8 weeks are needed to examine a longer term restoration of heart function post-MI. It is likely that the source of HGF is the transplanted SMB; however, it is unclear whether the source of other therapeutic cytokines is the transplanted cells, such as SMBs, MSCs, or both, or native cardiac cells.

In conclusion, we found that h-MSCs enhanced the paracrine effects of r-SMB sheets, thus enhancing angiogenesis, lowering fibrosis, inhibiting cellular hypertrophy, improving cardiac function, and prolonging cell survival in MI model

rats. These observations of improved effects from this co-cultured cell sheet may lead to new regeneration therapies for heart failure following advanced cardiomyopathy that are superior to the conventional SMB-only cell-sheet technique.

### Acknowledgments

We thank Dr. Eiji Kobayashi and Takashi Murakami for kindly providing the GFP transgenic Lewis rats. We thank Mr. Akima Harada, Mr. Shigeru Matsumi, and Mrs. Masako Yokoyama for their excellent technical assistance.

Sources of Funding: This study was supported by Grants for the Research and Development of the Myocardial Regeneration Medicine Program from the New Energy Industrial Technology Development Organization (NEDO), Japan. This research was supported by the Health and Labour Sciences Research Grants, Research on intractable diseases.

### Disclosure Statement

T.S. is a consultant for CellSeed, Inc. T.O. is an Advisory Board Member in CellSeed, Inc., and the inventor/developer designated on the patent for temperature-responsive culture surfaces.

### References

1. Menasche, P., Hagege, A.A., Scorsin, M., Puzet, B., Desnos, B., Schwartz, K., Vilquin, J.T., and Marolleau, J.P. Myoblast transplantation in heart failure. *Lancet* **357**, 279, 2001.
2. Hagege, A.A., Marolleau, J.P., Vilquin, J.T., Alheritiere, A., Peyrard, S., Duboc, D., Abergel, E., Messas, E., Mousseaux, E., Schwartz, K., Desnos, M., and Menasche, P. Skeletal myoblast transplantation in ischemic heart failure: Long-term follow-up of the first phase I cohort of patients. *Circulation* **114**, 1108, 2006.
3. Miyagawa, S., Roth, M., Saito, A., Sawa, Y., and Kostin, S. Tissue-engineered cardiac constructs for cardiac repair. *Ann Thorac Surg* **91**, 320, 2011.
4. Imanishi, Y., Miyagawa, S., Maeda, N., Fukushima, S., Kitagawa-Sakakida, S., Daimon, T., Hirata, A., Shimizu, T., Okano, T., Shimomura, I., and Sawa, Y. Induced adipocyte cell-sheet ameliorates cardiac dysfunction in a mouse myocardial infarction model: a novel drug delivery system for heart failure. *Circulation* **124**, S10, 2011.
5. Miyagawa, S., Saito, A., Sakaguchi, T., Yoshikawa, Y., Yamauchi, T., Imanishi, Y., Kawaguchi, N., Teramoto, N., Matsuura, N., Iida, H., Shimizu, T., Okano, T., and Sawa, Y. Impaired myocardium regeneration with skeletal cell sheets—a preclinical trial for tissue-engineered regeneration therapy. *Transplantation* **90**, 364, 2010.
6. Fujita, T., Sakaguchi, T., Miyagawa, S., Saito, A., Sekiya, N., Izutani, H., and Sawa, Y. Clinical impact of combined transplantation of autologous skeletal myoblasts and bone marrow mononuclear cells in patients with severely deteriorated ischemic cardiomyopathy. *Surg Today* **41**, 1029, 2011.
7. Sekiya, N., Matsumiya, G., Miyagawa, S., Saito, A., Shimizu, T., Okano, T., Kawaguchi, N., Matsuura, N., and Sawa, Y. Layered implantation of myoblast sheets attenuates adverse cardiac remodeling of the infarcted heart. *J Thorac Cardiovasc Surg* **138**, 985, 2009.
8. Memon, I.A., Sawa, Y., Fukushima, N., Matsumiya, G., Miyagawa, S., Taketani, S., Sakakida, S.K., Kondoh, H.,

- Aleshin, A.N., Shimizu, T., Okano, T., and Matsuda, H. Repair of impaired myocardium by means of implantation of engineered autologous myoblast sheets. *J Thorac Cardiovasc Surg* **130**, 646, 2009.
9. Matuura, K., Honda, A., Nagai, T., Fukushima, N., Iwanaga, K., Tokunaga, M., Shimizu, T., Okano, T., Kasanuki, H., Hagiwara, N., and Komuro, I. Transplantation of cardiac progenitor cells ameliorates cardiac dysfunction after myocardial infarction in mice. *J Clin Invest* **119**, 2204, 2009.
  10. Majumdar, M.K., Thiede, M.A., Mosca, J.D., Moorman, M., and Gerson, S.L. Phenotypic and functional comparison of cultures of marrow-derived mesenchymal stem cells (MSCs) and stromal cells. *J Cell Physiol* **176**, 57, 1998.
  11. Richards, M., Fong, C.Y., Chan, W.K., Wong, P.C., and Bongso, A. Human feeders support prolonged undifferentiated growth of human inner cell masses and embryonic stem cells. *Nat Biotechnol* **20**, 933, 2002.
  12. Ohkura, H., Matsuyama, A., Lee, C.M., Saga, A., Kakuta-Yamamoto, A., Nagao, A., Sougawa, N., Sekiya, N., Takekita, K., Shudo, Y., Miyagawa, S., Komoda, H., Okano, T., and Sawa, Y. Cardiomyoblast-like cells differentiated from human adipose tissue-derived mesenchymal stem cells improve left ventricular dysfunction and survival in a rat myocardial infarction model. *Tissue Eng Part C Methods* **16**, 417, 2010.
  13. Pittenger, M.F., Mackay, A.M., Beck, S.C., Jaiswal, R.K., Douglas, R., Mosca, J.D., Moorman, M.A., Simonetti, D.W., Craig, S., and Marshak, D.R. Multilineage potential of adult human mesenchymal stem cells. *Science* **284**, 143, 1999.
  14. Jiang, Y., Jahagrirar, B.N., Reinhardt, R.L., Schwartz, R.E., Keene, C.D., Ortiz-Gonzales, X.R., Reyes, M., Lenrik, T., Lund, T., Blackstad, M., Du, J., Aldrich, S., Lisberg, A., Low, W.C., Largaespada, D.A., and Vertaille, C.M. Pluripotency of mesenchymal stem cells derived from adult marrow. *Nature* **418**, 41, 2002.
  15. Inoue, H., Ohsawa, I., Murakami, T., Kimura, A., Hakamata, Y., Sato, Y., Kaneko, T., Takahashi, M., Okada, T., Ozawa, K., Francis, J., Leone, P., and Kobayashi, E. Development of new inbred transgenic strains of rats with LacZ or GFP. *Biochem Biophys Res Commun* **329**, 288, 2005.
  16. Kirouac Dc, and Zandstra, P.W. Understanding cellular networks to improve hematopoietic stem cell expansion cultures. *Curr Opin Biotechnol* **17**, 538, 2006.
  17. Germani, A., Di Carlo, A., Mangoni, A., Straino, S., Giacinti, C., Turrini, P., Biglioli, P., and Capogrosse, M.C. Vascular endothelial growth factor modulates skeletal myoblast function. *Am J Pathol* **163**, 1417, 2003.
  18. Sierra-Honigmann, M.R., Nath, A.K., Murakami, C., García-Cardeña, G., Papapetropoulos, A., Sessa, W.C., Madge, L.A., Schechner, J.S., Schwabb, M.B., Polverini, P.J., and Flores-Riveros, J.R. Biological action of leptin as an angiogenic factor. *Science* **281**, 1683, 1998.
  19. Hiesinger, W., Perez-Aguilar, J.M., Atluri, P., Marotta, N.A., Frederick, J.R., Fitzpatrick, J.R., 3rd, McCormick, R.C., Muenzer, J.R., Yang, E.C., Levit, R.D., Yuan, L.J., Macarthur, J.W., Saven, J.G., and Woo, Y.J. Computational protein design to reengineer stromal cell-derived factor-1 $\alpha$  generates an effective and translatable angiogenic polypeptide analog. *Circulation* **124**, S18, 2011.
  20. Frederick, J.R., Fitzpatrick, J.R., 3rd, McCormick, R.C., Harris, D.A., Kim, A.Y., Muenzer, J.R., Marotta, N., Smith, M.J., Cohen, J.E., Hiesinger, W., Atluri, P., and Woo, Y.J. Stromal cell-derived factor-1 $\alpha$  activation of tissue-engineered endothelial progenitor cell matrix enhances ventricular function after myocardial infarction by inducing neovascularogenesis. *Circulation* **122**, S107, 2010.
  21. Kakazu, A., Chandrasekher, G., and Bazan, H.E. HGF protects corneal epithelial cells from apoptosis by the PI-3K/Akt-1/Bad- but not the ERK 1/2-mediated signaling pathway. *Invest Ophthalmol Vis Sci* **45**, 3485, 2004.
  22. Sekine, H., Shimizu, T., Hobo, K., Sekiya, S., Yang, J., Yamato, M., Kurosawa, H., Kobayashi, E., and Okano, T. Endothelial cell coculture within tissue-engineered cardiomyocyte sheets enhances neovascularization and improve cardiac function of ischemic hearts. *Circulation* **118**, S145, 2008.
  23. Kobayashi, H., Shimizu, T., Yamato, M., Tono, K., Masuda, H., Asahara, T., Kasanuki, H., and Okano, T. Fibroblast sheets co-cultured with endothelial progenitor cells improve cardiac function of infarcted hearts. *J Artif Organs* **11**, 141, 2008.
  24. Miyahara, Y., Nagaya, N., Kataoka, M., Yanagawa, B., Tanaka, K., Hao, H., Ishino, K., Ishida, H., Shimizu, T., Kangawa, K., Sano, S., Okano, T., Kitamura, S., and Mori, H. Monolayered mesenchymal stem cells repair scarred myocardium after myocardial infarction. *Nat Med* **12**, 459, 2006.
  25. Risau, W. Mechanisms of angiogenesis. *Nature* **386**, 671, 1997.

Address correspondence to:

Yoshiki Sawa, MD, PhD

Department of Cardiovascular Surgery

Osaka University Graduate School of Medicine

Suita

Osaka 565-0871

Japan

E-mail: sawa-p@surg1.med.osaka-u.ac.jp

Received: September 2, 2012

Accepted: September 25, 2013

Online Publication Date: December 31, 2013

## Improvement of Cardiac Stem Cell Sheet Therapy for Chronic Ischemic Injury by Adding Endothelial Progenitor Cell Transplantation: Analysis of Layer-Specific Regional Cardiac Function

Sokichi Kamata,\* Shigeru Miyagawa,\* Satsuki Fukushima,\* Satoshi Nakatani,†  
Atsuhiko Kawamoto,‡ Atsuhiko Saito,\* Akima Harada,\* Tatsuya Shimizu,§  
Takashi Daimon,¶ Teruo Okano,§ Takayuki Asahara,‡ and Yoshiki Sawa\*

\*Department of Cardiovascular Surgery, Osaka University Graduate School of Medicine, Suita, Japan

†Division of Functional Diagnostics, Department of Cardiovascular Medicine,  
Osaka University Graduate School of Medicine, Suita, Japan

‡Division of Vascular Regeneration Therapy, Institute of Biomedical Research and Innovation, Kobe, Japan

§Institute of Advanced Biomedical Engineering and Science, Tokyo Women's Medical University, Tokyo, Japan

¶Department of Biostatistics, Hyogo College of Medicine, Nishinomiya, Hyogo, Japan

The transplantation of cardiac stem cell sheets (CSC sheets) is a promising therapeutic strategy for ischemic cardiomyopathy, although potential ischemia in the transplanted area remains a problem. Injected endothelial progenitor cells (EPCs) can reportedly induce angiogenesis in the injected area. We hypothesized that concomitant CSC sheet transplantation and EPC injection might show better therapeutic effects for chronic ischemic injury model than the transplantation of CSC sheets alone. Scaffold-free CSC sheets were generated from human c-kit-positive heart-derived cells. A porcine chronic ischemic injury model was generated by placing an ameroid constrictor around the left coronary artery for 4 weeks. The animals then underwent a sham operation, epicardial transplantation of CSC sheet over the ischemic area, intramyocardial injection of EPCs into the ischemic and peri-ischemic area, or CSC sheet transplantation plus EPC injection. The efficacy of each treatment was then assessed for 2 months. Speckle-tracking echocardiography was used to dissect the layer-specific regional systolic function by measuring the radial strain (RS). The epicardial RS in the ischemic area was similarly greater after treatment with the CSC-derived cell sheets alone ( $19 \pm 5\%$ ) or in combination with EPC injection ( $20 \pm 5\%$ ) compared with the EPC only ( $9 \pm 4\%$ ) or sham ( $7 \pm 1\%$ ) treatment. The endocardial RS in the ischemic area was greatest after the combined treatment ( $14 \pm 1\%$ ), followed by EPC only ( $12 \pm 1\%$ ), compared to the CSC only ( $11 \pm 1\%$ ) and sham ( $9 \pm 1\%$ ) treatments. Consistently, either epicardial CSC sheet implantation or intramyocardial EPC injection yielded increased capillary number and reduced cardiac fibrosis in the ischemic epicardium or endocardium, respectively. Concomitant EPC injection induced the migration of transplanted CSCs into the host myocardium, leading to further neovascularization and reduced fibrosis in the ischemic endocardium, compared to the CSC sole therapy. Transplantation of CSC sheets induced significant functional recovery of the ischemic epicardium, and concomitant EPC transplantation elicited transmural improvement in chronic ischemic injury.

Key words: Cardiac stem cells (CSCs); Endothelial progenitor cells (EPCs); Chronic ischemic injury; Strain imaging; Left ventricular remodeling

### INTRODUCTION

Transplantation of somatic tissue-derived stem cells has been shown to be a feasible, safe, and potentially effective treatment for advanced cardiac failure in clinical settings (6,32). In particular, cardiac stem cells (CSCs), represented by c-kit-positive cells in the myocardium, can play a central role in healing the damaged myocardium, through their direct differentiation in situ, the recruitment of circulating stem/progenitor cells, or the paracrine

release of cardioprotective factors (9,12,30). CSC transplantation is therefore considered a promising treatment for advanced cardiac failure, although the optimal method for cell delivery into the heart is still under debate (7).

The transplantation of scaffold-free cell sheets was shown to enhance the retention and survival of the transplanted cells and to minimize the risks of cell delivery-related myocardial damage that leads to arrhythmogenicity, thus showing good therapeutic potential (5,20,33). However,

Received July 26, 2012; final acceptance March 17, 2013. Online prepub date: April 3, 2013.

Address correspondence to Professor Yoshiki Sawa, Department of Cardiovascular Surgery, Osaka University Graduate School of Medicine, 2-2 Yamadaoka, Suita, Osaka 565-0871, Japan. Tel: +81-6-6879-3154; Fax: +81-6-6879-3163; E-mail: sawa-p@surg1.med.osaka-u.ac.jp

concerns remain regarding the integration of the transplanted cells into the myocardium, which would have a direct impact on regional cardiac function, and the potential for ischemia in the transplanted cell sheet, which would limit its therapeutic potential. On the other hand, endothelial progenitor cells (EPCs) have been shown to induce neoangiogenesis in the ischemic/infarcted myocardium and to activate residential CSCs to enhance healing and/or regeneration of the damaged myocardium (11,13,31). The intramyocardial injection of EPCs is thus another promising treatment for enhancing myocardial regeneration and possibly supporting the cellular function of transplanted CSCs (16).

We thus hypothesized that CSC transplantation by the cell sheet technique might induce cardiomyogenic differentiation in situ, reverse left ventricular (LV) remodeling, and improve functional recovery in ischemic injury model and that these therapeutic effects might be enhanced by the concomitant transplantation of EPCs, which could have different effects on the damaged myocardium from CSCs.

Several lines of evidence suggested that region-specific, especially layer-specific, LV function assessed by recently developing modalities may be superior to globally measured ejection fraction (EF) in predicting myocardial recovery after a wide range of medical and surgical treatment (3,14). Here we used a porcine chronic ischemic injury model to dissect the layer-specific functional effects of these two types of cell transplantation.

## MATERIALS AND METHODS

All human and animal studies were carried out with the approval of the institutional ethical committee. Human samples were collected under written informed consent. The investigation conforms to the Principles of Laboratory Animal Care formulated by the National Society for Medical Research and the NIH guidelines for the care and use of laboratory animals. All experimental procedures and evaluations were carried out in a blinded manner.

### *Isolation and Cultivation of C-Kit-Positive Cells From Human Cardiac Tissue*

Human normal right atrial tissues were obtained from a 53-year-old female patient with dilated cardiomyopathy at Osaka University Hospital. The isolation method was as published recently (6). Briefly, after dissecting fat and fibrous tissue, the sample was cut into small pieces (<1 mm<sup>3</sup>) and suspended in 8 ml Ham's F12 medium (Wako Pure Chemical Inc., Osaka, Japan) containing 0.2% collagenase (17454; Serva Electrophoresis, Heidelberg, Germany). After digestion, cells were plated in culture dishes (353003; BD Falcon, Franklin Lakes, NJ, USA) containing Ham's F12 supplemented with 10% fetal bovine serum (FBS; SH30406.02; Hyclone, Thermo Scientific,

Waltham, MA, USA), 10 ng/ml recombinant human basic fibroblast growth factor (bFGF; 100-18B; PeproTech, Rocky Hill, NJ, USA), 0.2 mM L-glutathione (G6013; Sigma-Aldrich, St. Louis, MO, USA), and 5 mU/ml erythropoietin (E5627-10UN; Sigma Aldrich). Subsequently, cells were expanded and subjected to fluorescence-activated cell sorting (FACSARIA; BD Biosciences, San Jose, CA, USA) with antibody {cluster of differentiation 117-phycoerythrin [CD117(AC126)-PE]; also known as c-kit or stem cell growth factor receptor, 130-091-735; Miltenyi Biotec, Bergisch Gladbach, Germany} to obtain c-kit-positive CSCs. The sorted c-kit-positive CSCs were cultured until the fifth passage in the above medium (30).

### *Preparation of CSC Sheet and Endothelial Progenitor Cells*

Cultured CSCs were characterized by fluorescence-activated cell sorting (FACS) analysis, labeled by 2  $\mu$ M DiI-red (Molecular Probes, Eugene, OR, USA) (33), and then incubated on 10-cm thermoresponsive dishes (Cell Seed Inc., Tokyo, Japan) at 37°C for 12 h. The DiI-red-labeled CSCs spontaneously detached from the dish surface following incubation at 20°C for 30 min, yielding a CSC sheet. Each CSC sheet was approximately 42 mm in diameter and 100  $\mu$ m thick. Granulocyte colony-stimulating factor-mobilized EPCs of human origin (AllCells, MPB-017F; Emeryville, CA, USA) were labeled with 2  $\mu$ M DiI-blue in vitro (Molecular Probes) (33). The following monoclonal antibodies were used: c-kit allophycocyanin (APC) [A3C6E2 (clone), 130-091-733; MiltenyiBiotec], CD105 PE (FAB10971P; R&D Systems, Minneapolis, MN, USA), CD34 fluorescein isothiocyanate (FITC) (555821, BD Biosciences), CD31 PE (FAB3567P, R&D Systems), 7-aminoactinomycin D peridinin-chlorophyll protein-cyanine 5.5 [7AAD PerCP-Cy5-5; 51-68981E (559925); BD Biosciences], immunoglobulin G1(IgG1)-FITC isotype controls (555748; BD Biosciences), IgG1-APC isotype controls (130-092-214; Miltenyi Biotec), and IgG1-PE isotype controls (IC002P; R&D Systems).

### *Generation of the Swine Chronic Ischemic Injury Model and Cell Transplantation*

A 2.5-mm ameroid constrictor (Tokyo Instruments, Inc., Tokyo, Japan) was placed around the proximal left anterior descending artery via a left thoracotomy in female swine (Clawn miniature, 1 year old, 25 kg; Japan Farm, Inc., Kagoshima, Japan). A total of 65 swines were then cared for in a temperature-controlled individual cage with a daily intake of 5 mg/kg cyclosporin A (Novartis, East Hanover, NJ, USA) (15). Multidetector CT identified 52 pigs that developed a left ventricular ejection fraction (LVEF) between 30% and 40% at 21 days post-ameroid placement. Since eight of these pigs died prior to cell transplantation, a total of 44 pigs were randomly divided

into four treatment groups ( $n = 11$  in each): sham operation (sham group), CSC sheet transplantation only (CSC-only group), intramyocardial injection of EPCs (EPC-only group), and CSC sheet transplantation plus EPC injection (CSC–EPC group). After a median sternotomy under general anesthesia, three-layered CSC sheet (total  $1 \times 10^8$  cells) was placed on the epicardium of the ischemic area [left anterior descending (LAD) region] and stitched in place around the edge. EPCs (total  $2.5 \times 10^6$  cells) were intramyocardially injected into 12 different sites of the ischemic and peri-ischemic area. After the transplantation and/or intramyocardial injection was completed, the pericardium was closed. The pigs were taken care of for 1 day ( $n = 1$  each), 3 weeks ( $n = 4$  each), or 8 weeks ( $n = 6$  each), when they were sacrificed in a humane manner.

#### *Continuous Electrocardiogram Monitoring*

The electrocardiogram (ECG) was monitored during 5 days posttreatment with the Holter system (Unique Medical Co., Tokyo, Japan) for swines sacrificed at 8 weeks after cell transplantation ( $n = 6$  each group). The heart rate and arrhythmia events during the first 24 h were analyzed using software (Softron Co., Tokyo, Japan).

#### *Multidetector CT and Conductance Catheterization*

Global LV function was assessed by multidetector computed tomography (CT) at pretreatment and 8 weeks posttreatment ( $n = 6$  each) and by cardiac catheterization at 8 weeks posttreatment ( $n = 5$  each). After infusing 45 ml of nonionic contrast agent (Iomeron 350; Eisai Co., Tokyo, Japan) via the ear vein, 5-mm slice images of the entire heart were obtained in the craniocaudal direction using a 16-slice CT scanner (Emotion 16; Siemens, Tokyo, Japan). Every 10% of the R-R interval was reconstructed to calculate the LVEF and end-diastolic/systolic volume (EDV and ESV, respectively) using software (Lexus, Aze Inc., Tokyo, Japan).

Pressure–volume (P–V) cardiac catheterization was performed after median sternotomy by inserting a conductance catheter (Unique Medical) and a microtip catheter transducer (SPR-671; Millar Instruments, Inc., Houston, TX, USA) into the LV cavity. The P–V loop data under stable hemodynamics or inferior vena cava occlusion were analyzed with Integral 3 software (Unique Medical).

#### *Speckle-Tracking Echocardiography and Myocardial Contrast Echocardiography*

Short-axis echocardiographic images, obtained using the Artida 4D Echocardiography System (Toshiba Medical Systems Co., Tochigi, Japan) and PST-30SBT transducer, were analyzed by the speckle-tracking method using wall motion-tracking software (Toshiba Medical Systems) (2,4). End-systolic radial strain (RS) values at the mid and apical levels were averaged in a layer-specific manner to

measure the endocardial and epicardial wall motion index (WMI), respectively.

Myocardial contrast echocardiography was performed using real-time contrast pulse sequencing operating on the Aplio ultrasound system (Toshiba Medical Systems) (8). Briefly, after an intravenous injection of 20 ml of ultrasound contrast agent (Sonazoid, Daiichi Sankyo Inc., Parsippany, NJ, USA), images in the apical two-chamber view were acquired to score the myocardial opacification using Volmac software (YD Ltd., Nara, Japan).

#### *Histology*

Cultured CSCs on eight-well Lab-Tec chamber slides were fixed with 4% paraformaldehyde (163-20145, Wako Pure Chemical Inc.), labeled, and examined by confocal microscopy (FV300, Olympus, Tokyo, Japan). Alexa Fluor-488 phalloidin (Molecular Probes) was used to enhance the background actin filaments. Paraffin-embedded transverse sections at the papillary muscle level were stained with Masson's trichrome (MT; Masson's Trichrome staining kit, Muto Pure Chemicals, Tokyo, Japan), and the amount of interstitial collagen at the entire LV wall was semi-quantified by MetaMorph software (Molecular Devices, Sunnyvale, CA, USA) ( $n = 6$ , in each). In addition, the thickness of the ventricular wall was measured at two points from the LV posterior area and two points from the interventricular septum, and results were expressed as the average of the four points. Five-micrometer cryosections were subjected to either periodic acid-Schiff (PAS) staining (PAS staining kit, Muto Pure Chemicals) or immunohistochemical labeling. The following primary antibodies were used: rabbit anti-c-kit (1:50; Dako Co., Glostrup, Denmark), rabbit anti-von Willebrand factor (vWF; 1:500; Dako), mouse anti-Ki-67 (1:50; Dako), rabbit anti-connexin 43 (1:200; Sigma Aldrich), mouse anti-cardiac troponin I (cTn-I; 1:100; Abcam Co., Cambridge, UK), mouse anti-stromal cell-derived factor 1 (SDF-1; 1:50; Abcam), rabbit anti-vascular endothelial growth factor (VEGF; 1:100; Thermo Scientific), and rabbit anti-insulin-like growth factor 1 (IGF-1; 1:100; Abcam). Capillary density was expressed as the average number of vWF-positive circular structures in five randomly selected sections, corrected for the total area of the tissue section measured. PAS-stained sections were used to determine the cell diameter of the cardiomyocytes at the remote zone. DiI-red-positive cells were traced by MetaMorph software to quantify the area of engrafted clusters of CSC sheet.

#### *Reverse Transcription Polymerase Chain Reaction (RT-PCR)*

Total RNA was extracted from the CSCs and the swine heart tissues posttreatment using an RNeasy Kit (Qiagen, Hilden, Germany), then reverse-transcribed using Omniscript Reverse Transcriptase (Qiagen) and

amplified using the Gene Amp<sup>®</sup> PCR System 9700 (Life Technologies, Tokyo, Japan). The primer pairs were as follows: human-specific kinase insert domain receptor (KDR or VEGF receptor 2) primer sequence, sense CCT CTA CTC CAG TAA ACC TGA TTG GG, antisense TGT TCC CAG CAT TTC ACA CTA TGG; human-specific chemokine C-X-C motif receptor 4 [CXCR4 or stromal-derived factor 1 (SDF-1) receptor] primer sequence, sense ACG TCA GTG AGG CAG ATG, antisense GAT GAC TGT GGT CTT GAG; human glyceraldehyde-3-phosphate dehydrogenase (GAPDH) primer sequence, sense AAT GGG CAG CCG TTA GGA AA, antisense GCG CCC AAT ACG ACC AAA TC; swine-specific SDF-1 primer sequence, sense CCGAACTGTGCCCTTCAGAT, antisense ATAA ACATCCCGCCGTCCTC; swine-specific CXCR-4 primer sequence, sense GCGCAAAGCTCTCAAACCA, antisense CAGTGGA AAAAGGCAAGGGC; swine-specific VEGF primer sequence, sense GAC GTC TAC CAG CGC AGC TAC T, antisense TTT GAT CCG CAT AAT CTG CAT G; swine-specific IGF-1 primer sequence, sense ACA TCC TCT TCG CAT CTC TTC TAC TT, antisense CCA GCT CAG CCC CAC AGA; swine GAPDH primer sequence, sense CTG CAC CAC CAA CTG CTT AGC, antisense GCC ATG CCA GTG AGC TTC C. The transcript level of GAPDH was used as an endogenous reference. The products from the cultured CSCs were stained with ethidium bromide (Bio-Rad Laboratories, Hercules, CA, USA), separated by electrophoresis (Mupid submarine electrophoresis system, Advance Co. Ltd., Tokyo, Japan) on an agarose gel (Agarose S, Nippon Gene Co., Ltd., Tokyo, Japan), and quantified.

#### *Fluorescence In Situ Hybridization (FISH)*

Paraffin-embedded sections were predenatured, dehydrated, and then labeled with deoxyribonucleic acid probes, a Cy3-conjugated probe for human-specific genome, Cy5-conjugated probe for swine-specific genome (Chromosome Science Laboratory, Hokkaido, Japan), and mouse anti-cTn-I or rabbit anti-vWF. The sections were visualized with secondary antibodies conjugated to Alexa fluorochromes. Nuclei were labeled with 4,6-diamino-2-phenylindole (DAPI; Molecular Probes).

#### *Statistical Analysis*

Continuous data are summarized as medians with ranges (minimums to maximums) or means  $\pm$  SEM (standard error of mean) and are plotted in figures with raw values or barplots of the means with symmetric SEM bars, as appropriate. Distributions of the continuous data were checked for normality with the Shapiro–Wilk test and for equality of between-group variances with the Levene test. Normally distributed data were compared between four groups using the analysis of variance (ANOVA), followed by the Tukey multiple comparison for equal variances, or Welch's

ANOVA, followed by the Games–Howell multiple comparison for unequal variances. Nonnormally distributed data were compared using the Kruskal–Wallis test, followed by the Steel–Dwass multiple comparison. Normally and nonnormally distributed data before and after treatment were compared using the paired *t* test and the Wilcoxon signed rank-sum test, respectively. All *p* values are two-sided, and values of *p* < 0.05 were considered to indicate statistical significance. All analyses were performed with the SPSS 11.0J for Windows (SPSS, Chicago, IL, USA) and the R program (<http://www.r-project.org/>) (10).

## RESULTS

### *Human Atrium-Derived C-Kit-Positive Cells Showed CSC Characteristics In Vitro*

The isolated right atrium-derived cells were characterized *in vitro* by FACS, immunohistolabeling, and RT-PCR analyses. The proportion of c-kit-positive cells at the second passage was  $99 \pm 4\%$  (Fig. 1A and B). However, as the cells expanded, they lost the primitive phenotype, and more than half of them had the potential to differentiate to the endothelial rather than the cardiomyocyte or smooth muscle cell lineage. The proportion of c-kit-positive cells at the fifth passage was  $20 \pm 10\%$ , while 34%, 71%, and 99% of them expressed CD34, CD31, and CD105, respectively (Fig. 1C). Immunohistochemistry revealed that approximately 5% of the cells expressed cTn-I in the cytoplasm (Fig. 1D). In addition, RT-PCR clearly revealed the expression of CXCR4 and KDR in the cells (Fig. 1E).

After incubating the cells on temperature-responsive dishes at 37°C for 12 h, CSC sheets were generated by lowering the temperature. Each cell sheet was approximately 42 mm in diameter, and the gap junction protein connexin 43 was expressed between the cells (Fig. 1F). Most of the cells expressed the proliferation marker Ki-67 in their nucleus (Fig. 1G).

### *Successful Cell Transplantation With Minimal Arrhythmogenicity*

A total of 44 pigs underwent treatment, which was performed without any procedure-related mortalities (*n* = 11 each). Fatal arrhythmias, such as ventricular tachycardia and fibrillation, or composite ventricular arrhythmias (grades 3–5 in Lown's classification) were not detected in any group during the first 24 h posttreatment, as assessed by Holter ECG monitoring (*n* = 6 each) (Table 1). There were no significant differences in the heart rate or number of unifocal premature ventricular/atrial contractions among the groups.

### *Global Functional Recovery After CSC Sheet Transplantation Was Enhanced by EPC Injection*

Multidetector CT measured LVESV, LVEDV, and LVEF, and cardiac catheterization measured the systolic

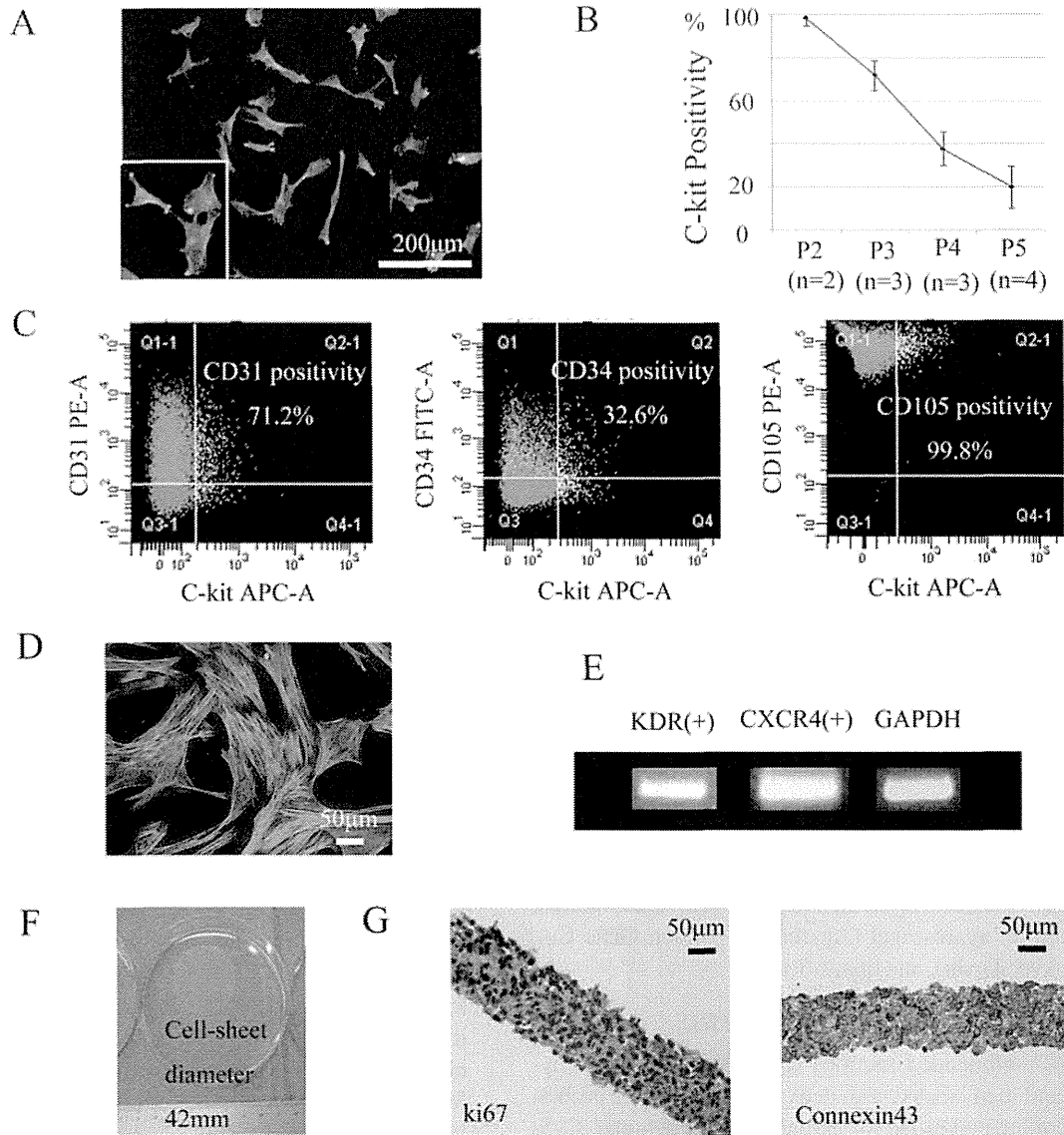


**Figure 1.** Characterization of the CSC sheet in vitro. (A) Representative double immunostaining for c-kit (red) and phalloidin (green) of cultured CSCs at the second passage. (B) C-Kit positivity was markedly decreased by passage culture. (C) FACS analysis of cultured CSCs at the fifth passage. (D) Cultured CSCs at the fifth passage expressed myocyte structural protein, a characteristic of cardiac progenitor cells. Phalloidin (green), troponin I (red). (E) RT-PCR analysis of CSCs at the fifth passage. (F) Detached CSC sheet. (G) Representative immunostaining for Ki-67 or connexin 43. Nuclear staining by DAPI is shown in blue in (A) and (D). Abbreviations: CSC, cardiac stem cell; FACS, fluorescence-activated cell sorting; CD31, cluster of differentiation 31; RT-PCR, reverse transcription polymerase chain reaction; KDR, kinase insert domain receptor; CXCR4, chemokine C-X-C motif receptor 4; GAPDH, glyceraldehyde 3-phosphate dehydrogenase; DAPI, 4,6-diamino-2-phenylindole.

**Table 1.** Evaluation of Fatal Arrhythmia by 24-h ECG Monitoring Posttransplantation

Group	Heart Rate (bpm)			PAC	PVC				VT	Vf
	Max Beat	Min Beat	Mean Beat		Singlet	Couplet	Triplet			
Sham (n=6)	181 ± 42	83 (52–118)	102 (62–137)	208 (126–297)	35 (6–65)	0	0	0	0	
EPC-only (n=6)	189 ± 31	100 (53–132)	113 (71–163)	254 (102–377)	55 (21–83)	0	0	0	0	
CSC-only (n=6)	171 ± 29	55 (50–79)	97 (45–101)	120 (44–201)	19 (9–58)	0	0	0	0	
CSC-EPC (n=6)	172 ± 17	83 (42–92)	101 (48–169)	250 (145–377)	48 (15–77)	0	0	0	0	

Abbreviations: ECG, electrocardiogram; PAC, premature atrial contraction; PVC, premature ventricular contraction; VT, ventricular tachycardia; Vf, ventricular fibrillation; EPC, endothelial progenitor cell; CSC, cardiac stem cell.

parameters  $dP/dt$  max, end-systolic pressure–volume relation (ESPVR), and diastolic parameters:  $\tau$ , end-diastolic pressure (EDP), and  $dP/dt$  min. There were no significant differences in LVESV, LVEDV, or LVEF among the group pretreatment (Fig. 2A–C). The pigs treated with the sham operation developed increases in LVESV ( $p < 0.001$ ) and LVEDV ( $p < 0.001$ ) but not in LVEF ( $34 \pm 5\%$  to  $32 \pm 6\%$ ,

$p = 0.44$ ) in 8 weeks. In contrast, the pigs in the EPC-only or CSC-only group showed preserved LVESV (EPC-only,  $p = 0.23$ ; CSC-only,  $p = 0.89$ ), LVEDV (EPC-only,  $p = 0.15$ ; CSC-only,  $p = 0.13$ ), and LVEF (EPC-only,  $37 \pm 5\%$  to  $37 \pm 4\%$ ,  $p = 0.91$ ; CSC-only,  $36 \pm 4\%$  to  $43 \pm 5\%$ ,  $p = 0.12$ ). Moreover, the combined treatment induced a significant decrease in LVESV ( $p = 0.04$ ) and a significant increase in

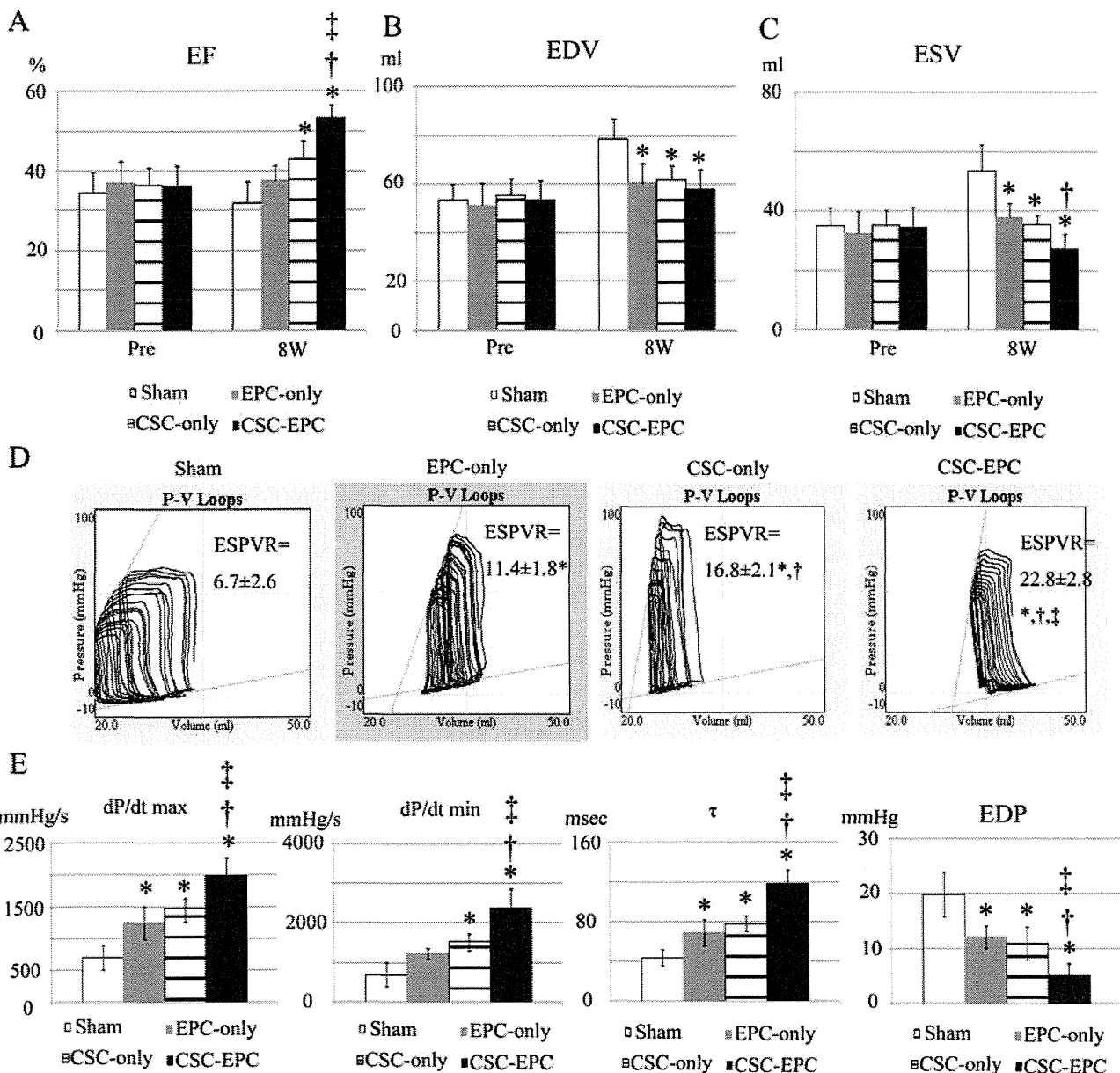


**Figure 2.** Global LV function assessed by multidetector CT and conductance catheter. (A–C) Multidetector CT parameters [(A) EF, (B) EDV, (C) ESV] before and 8 weeks after cell transplantation ( $n = 6$  each). (D) Representative P–V loops during IVC occlusion for each group at 8 weeks posttreatment ( $n = 5$  each). ESPVR of the CSC–EPC group was the greatest followed by that of the CSC-only group, then the EPC-only group, and then the sham group ( $p < 0.001$ , ANOVA). (E)  $dP/dt$  max,  $dP/dt$  min,  $\tau$  and EDP ( $n = 5$  each). \* $p < 0.05$  versus sham, † $p < 0.05$  versus EPC-only, ‡ $p < 0.05$  versus CSC-only. Abbreviations: LV, left ventricle; CT, computed tomography; EF, ejection fraction; EDV, end-diastolic volume; ESV, end-systolic volume; P–V, pressure–volume; IVC, inferior vena cava; ESPVR, end-systolic pressure–volume relationship; CSC, cardiac stem cell; EPC, endothelial progenitor cell; EDP, end-diastolic pressure.

LVEF ( $36 \pm 5\%$  to  $53 \pm 3\%$ ,  $p=0.001$ ) in the 8 weeks following cell transplantation.

At 8 weeks posttreatment, the LVESV of the CSC-only and EPC-only groups was significantly smaller than that of the sham group, and the LVESV of the CSC-EPC group was even smaller than that of the EPC-only group ( $p<0.001$  for CSC-EPC, CSC-only, and EPC-only vs. sham, and for CSC-EPC vs. EPC-only). The LVEDV of the CSC-EPC, CSC-only, and EPC-only groups was significantly smaller than that of the sham group ( $p=0.001$  for CSC-EPC, CSC-only, and EPC-only vs. sham). The LVEF of the CSC-only group was significantly greater than that of the sham group, while the LVEF of the CSC-EPC group was even greater than that of the other groups ( $p<0.001$  for CSC-EPC vs. CSC-only, EPC-only, and sham, and for CSC-only vs. sham). Moreover, the ESPVR of the CSC-EPC group was the greatest, followed by that of the CSC-only group, then the EPC-only group, and then the sham group (Fig. 2D).

The  $dP/dt$  max,  $\tau$ , EDP, and absolute value of  $dP/dt$  min were significantly greater in the CSC-EPC group than in the CSC-only and EPC-only groups, and these values except for the absolute value of  $dP/dt$  min were significantly greater in the CSC-only and EPC-only groups than in the sham group (Fig. 2E).

#### *Differential Region- or Layer-Specific Effects by CSC and EPC Transplantation*

Region- or layer-specific systolic LV function was assessed using speckle-tracking echocardiography, which was carried out at pretreatment and at 4 and 8 weeks posttreatment ( $n=6$ ). There was no significant difference in the endocardial or epicardial wall motion index in the ischemic anterior area among the groups at pretreatment (Fig. 3A and B).

The pigs given the sham operation developed a significant decrease in the epicardial wall motion index ( $10 \pm 2\%$  to  $7 \pm 1\%$ ,  $p=0.01$ ) and no change in the endocardial wall motion index ( $10 \pm 1\%$  to  $9 \pm 1\%$ ,  $p=0.40$ ) in 8 weeks. In contrast, cell transplantation induced a significant increase in epicardial [CSC-only,  $10 \pm 2\%$  to  $18$  ( $14$ – $28$ )%,  $p=0.03$ ; CSC-EPC,  $10 \pm 1\%$  to  $20 \pm 5\%$ ,  $p=0.01$ ] and endocardial (EPC-only,  $10 \pm 1\%$  to  $12 \pm 1\%$ ,  $p=0.01$ ; CSC-EPC,  $10 \pm 1\%$  to  $14 \pm 1\%$ ,  $p=0.001$ ) indices at 8 weeks.

At 8 weeks posttreatment, the epicardial wall motion index of the CSC-EPC and CSC-only groups was significantly greater than that of the EPC-only or sham group ( $p<0.001$  for CSC-EPC and CSC-only vs. EPC-only and sham) (Fig. 3A and C). In contrast, the endocardial wall motion index of the CSC-EPC group was the greatest followed by that of the EPC-only group, and both were significantly greater than that of the CSC-only or sham group ( $p<0.001$  for CSC-EPC vs. EPC-only vs. CSC-only and sham) (Fig. 3B and D).

Consistent with these findings, the myocardial perfusion score in the ischemic zone at 8 weeks posttreatment was significantly greater in the CSC-EPC ( $36 \pm 1$  dB) than in the sham group ( $19 \pm 2$  dB,  $p<0.001$ ) (Fig. 3E and F).

#### *Engraftment of Transplanted CSCs and EPCs and Neovascularization of the Infarcted Wall*

The engraftment of transplanted DiI-red-labeled CSCs and DiI-blue-labeled EPCs was examined, and the capillary density was assessed by fluorescence-based immunohistology for vWF. At 3 weeks after cell transplantation, most of the transplanted CSCs were present over the ischemic area in the sheet shape, although no DiI-red- or DiI-blue-positive cells could be seen in any heart slice at 8 weeks posttreatment (Fig. 4A and B). The number of vWF-positive capillaries in the ischemic epicardium of the CSC-EPC and CSC-only groups was significantly greater than in the EPC-only or sham group (CSC-EPC,  $251 \pm 84/\text{mm}^2$ ; CSC-only,  $257 \pm 43/\text{mm}^2$ ; EPC-only,  $105 \pm 20/\text{mm}^2$ ; sham,  $112 \pm 23/\text{mm}^2$ ;  $p=0.001$  for CSC-EPC and CSC-only vs. EPC-only and sham) (Fig. 4C). In contrast, the number of capillaries in the ischemic endocardium was significantly greatest in the CSC-EPC, followed by the EPC-only group, and then by the CSC-only or sham group (CSC-EPC,  $269 \pm 11/\text{mm}^2$ ; EPC-only,  $193 \pm 14/\text{mm}^2$ ; CSC-only,  $108 \pm 30/\text{mm}^2$ ; sham,  $74 \pm 38/\text{mm}^2$ ;  $p<0.001$  for CSC-EPC vs. EPC-only vs. CSC-only and sham). In association with these findings, some of the transplanted CSCs in both the CSC-EPC and CSC-only groups were observed in native epicardial tissues, while some had migrated into the endocardial tissues only in the CSC-EPC group (Fig. 4D). On the other hand, transplanted EPCs in both the CSC-EPC and EPC groups were observed in the ischemic and peri-ischemic area of the endocardium, especially near the vascular wall.

To elucidate the possible mechanism for the transplanted CSC migration, RT-PCR and immunostaining for angiogenic growth factors were performed ( $n=4$  each). The mRNA levels of swine-specific SDF-1, VEGF, and IGF-1 were upregulated in all the treatment groups (Fig. 5A). In particular, the mRNA levels of SDF-1 and the SDF-1 receptor CXCR4 were markedly greater in the CSC-EPC group than in the other groups (SDF-1 or CXCR4:  $p<0.001$  for CSC-EPC vs. CSC-only, EPC-only, and sham). In addition, SDF-1, but not VEGF or IGF-1, was expressed in the cytoplasm of the transplanted CSCs that were present in the native myocardial tissue in the CSC-EPC group (Fig. 5B).

#### *Preserved Myocardial Integrity 8 Weeks After Cell Transplantation*

Interstitial fibrosis and capillary density in the heart at 8 weeks posttreatment were assessed by MT (Fig. 6A) and PAS (Fig. 6B) staining and immunohistology for vWF (Fig. 6C), respectively ( $n=6$  each). Excluding

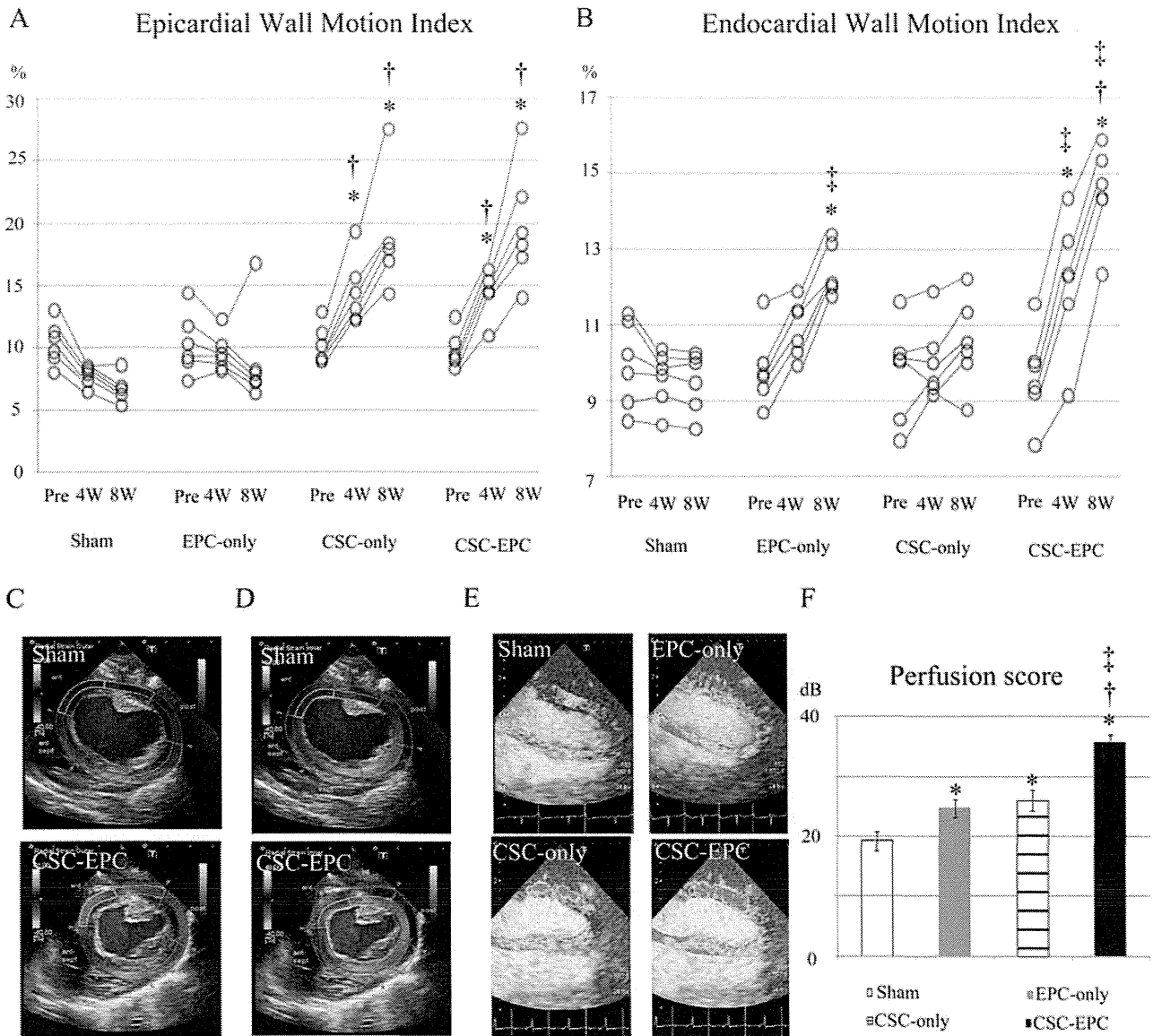


**Figure 3.** Region- and layer-specific systolic LV function and myocardial perfusion assessed by speckle-tracking and real-time contrast echocardiography. (A, B) Epicardial (A) and endocardial (B) WMIs in the ischemic area before, 4 and 8 weeks after cell transplantation ( $n=6$  each). At 8 weeks posttreatment, the epicardial WMI of the CSC-EPC and CSC-only groups was significantly greater than that of the EPC-only or sham group ( $p=0.001$ , Kruskal-Wallis test), while the endocardial WMI of the CSC-EPC group was the greatest followed by that of the EPC-only group, and then the CSC-only and sham group ( $p<0.001$ , ANOVA). (C, D) Representative epicardial (C) and endocardial (D) radial strain images at end-systole in the CSC-EPC and sham groups. (E) Representative contrast echocardiography 2D-imaging visualized by Volmac software in each group. (F) Myocardial perfusion scores 8 weeks posttreatment ( $n=6$ ). Myocardial perfusion score in the ischemic zone was significantly greater in the CSC-EPC than in the sham group ( $p<0.001$ , ANOVA) \* $p<0.05$  versus sham, † $p<0.05$  versus EPC-only, ‡ $p<0.05$  versus CSC-only. Abbreviations: LV, left ventricular; 2D, two-dimensional; CSC, cardiac stem cell; EPC, endothelial progenitor cell; WMI, wall motion index.

the sham group, there were no significant differences in infarct area among the other groups. On the other hand, the accumulation of collagen or area of chronic ischemic injury was the smallest in the CSC-EPC group followed by the CSC-only and EPC-only groups, and then by the sham group (CSC-EPC,  $7 \pm 1\%$ ; CSC-only,  $15 \pm 3\%$ ; EPC-only,  $20 \pm 3\%$ ; sham  $28 \pm 5\%$ ;  $p<0.001$  for CSC-EPC

vs. CSC-only and EPC-only vs. sham) (Fig. 6D). The LV wall thickness was significantly larger in the CSC-EPC group than in the sham group (CSC-EPC,  $9 \pm 1$  mm; sham  $7 \pm 1$  mm;  $p<0.01$  for CSC-EPC vs. sham) (Fig. 6E).

The myocyte cell diameter at 8 weeks posttreatment was assessed in the 5-mm heart sections of the remote zone stained by PAS ( $n=6$  each). The myocyte diameter

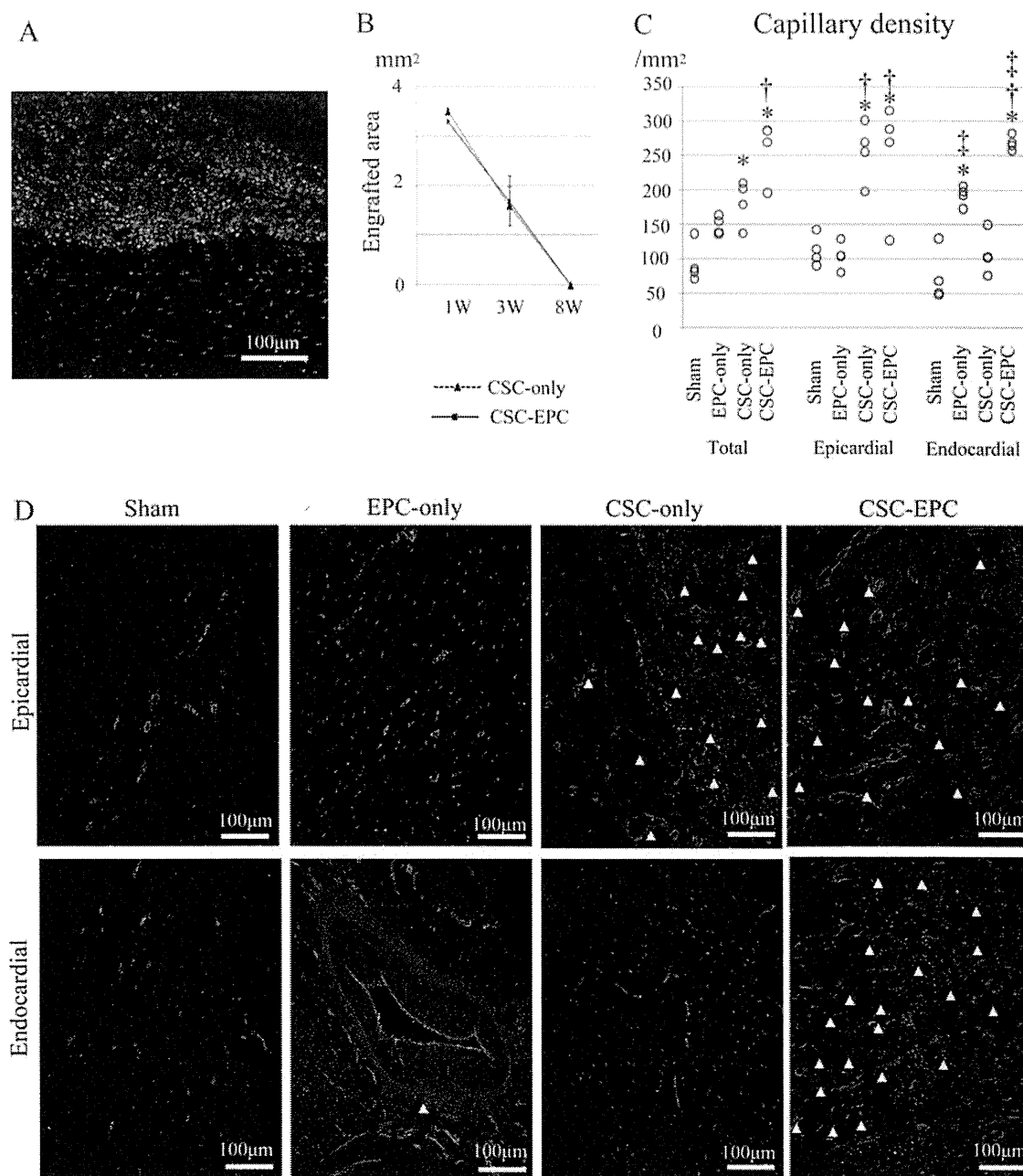


**Figure 4.** Engraftment of transplanted CSCs and EPCs and neovascularization of the ischemic wall. (A) Engraftment of the transplanted DiI-red-labeled CSC sheets (red) at 3 weeks posttreatment. (B) Quantification of the CSC sheet engrafted area in the CSC-only and CSC-EPC groups 1, 3, and 8 weeks posttreatment. (C) Quantification of the vWF-positive capillary density at the ischemic epicardium and endocardium in each group at 3 weeks posttreatment. The number of vWF-positive capillaries in the ischemic epicardium of the CSC-EPC and CSC-only groups was significantly greater than in the EPC-only or sham group ( $p < 0.001$ , ANOVA), while the number of capillaries in the ischemic endocardium was significantly greatest in the CSC-EPC, followed by the EPC-only group, and then by the CSC-only and sham groups ( $p < 0.001$ , ANOVA). (D) Representative immunostaining for vWF (green) at the ischemic epicardium and endocardium at 3 weeks posttreatment in each group. Migration of CSCs into the ischemic endocardium was observed only in the CSC-EPC group, and not in the CSC-only group. Yellow and white arrows indicate CSCs and EPCs, respectively.  $*p < 0.05$  versus sham,  $†p < 0.05$  versus EPC-only,  $‡p < 0.05$  versus CSC-only. Nuclear staining by DAPI is shown in blue in (A) and (D). Abbreviations: CSC, cardiac stem cell; vWF, von Willebrand factor.

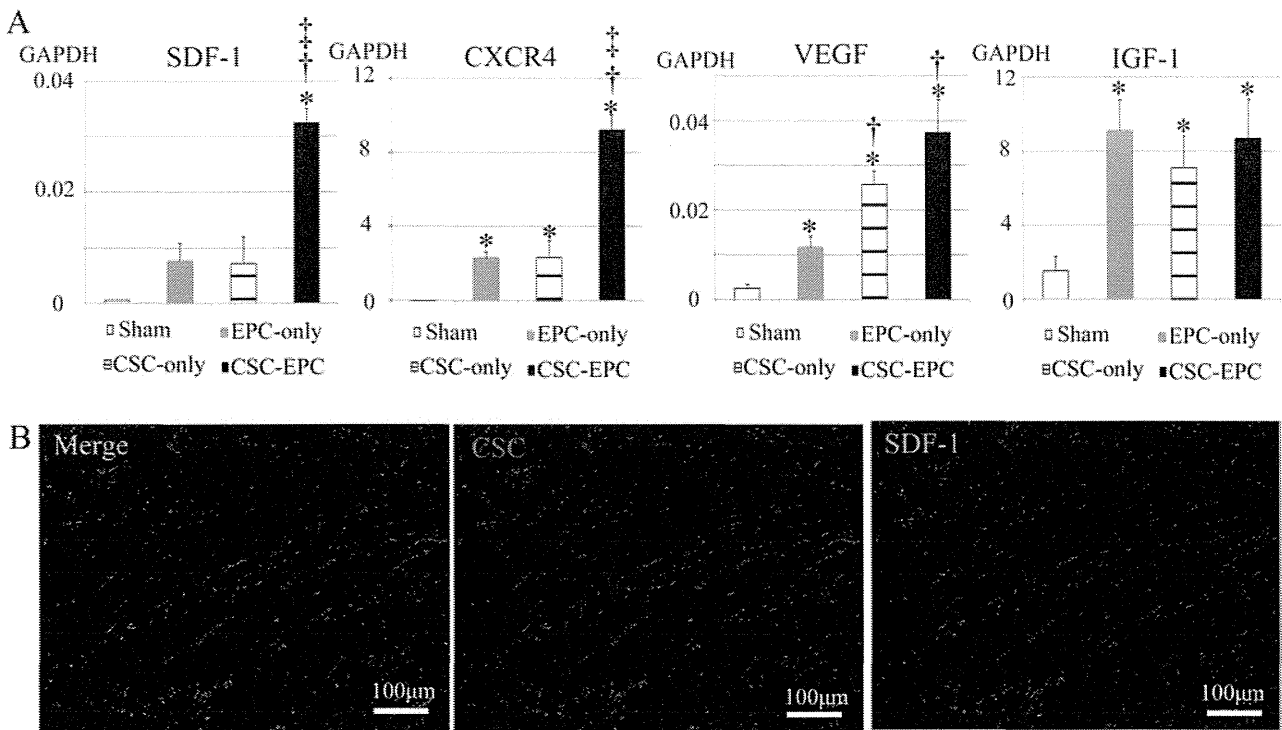


**Figure 5.** Possible mechanism of CSC migration. (A) RT-PCR analysis in each group at 3 weeks posttreatment. The mRNA levels of swine-specific SDF-1 ( $p < 0.001$ , Welch's ANOVA) and CXCR4 ( $p < 0.001$ , Welch's ANOVA) were markedly greater in the CSC-EPC group than in the other groups ( $n = 4$  each). (B) Representative immunostaining for SDF-1 in the CSC-EPC group at 3 weeks posttreatment. DiI-red-labeled CSCs (middle panel), SDF-1 (green) (right panel), and merged image (left panel). Nuclear staining by DAPI is shown in blue. \* $p < 0.05$  versus sham, † $p < 0.05$  versus EPC-only, ‡ $p < 0.05$  versus CSC-only. Abbreviations: CSC, cardiac stem cell; RT-PCR, reverse transcription polymerase chain reaction; SDF-1, stromal cell-derived factor 1; CXCR4, chemokine C-X-C motif receptor type 4; EPC, endothelial progenitor cell; GAPDH, glyceraldehyde 3-phosphate dehydrogenase; VEGF, vascular endothelial growth factor; IGF-1, insulin-like growth factor-1.

was significantly smaller in the CSC-EPC group than in the CSC-only, the EPC-only, or the sham group (CSC-EPC,  $33 \pm 9$  mm; CSC-only,  $49 \pm 10$  mm; EPC-only,  $55 \pm 8$  mm; sham  $61 \pm 8$  mm;  $p < 0.001$  for CSC-EPC vs. CSC-only, EPC-only, and sham) (Fig. 6F).

The number of vWF-positive capillaries in the peri-ischemic zone of the CSC-only or EPC-only group was greater than that of the sham group, and the number of the CSC-EPC group was even greater than that of the EPC-only or sham group. (CSC-EPC,  $83 \pm 11/\text{mm}^2$ ; CSC-only,  $74 \pm 6/\text{mm}^2$ ; EPC-only,  $62 \pm 8/\text{mm}^2$ ; sham  $32 \pm 10/\text{mm}^2$ ;  $p < 0.001$  for CSC-only and EPC-only vs. sham, and for CSC-EPC vs. EPC-only and sham) (Fig. 6G). In addition, greater vessel formation with vascular lumen was induced in the CSC-EPC group compared with the other groups.

#### Phenotypic Fate of Transplanted CSCs and EPCs Posttransplantation

The phenotype of the transplanted CSCs and EPCs in the native myocardium at 8 weeks posttransplantation was histologically assessed by human- and/or swine-specific genome-based FISH analysis. Small numbers

of cardiomyocytes and endothelial cells with a human genome in the nucleus were present in the native myocardium of both the CSC-EPC and CSC-only groups, but not in the EPC-only group (Fig. 7A and B). However, there was no difference in the number of cells with a human genome between the CSC-EPC and CSC-only groups. Of note, all the cells with a human genome in the nucleus also carried a swine genome in the nucleus and thus had chimeric nuclei (Fig. 7C and D).

## DISCUSSION

We here demonstrated that primary c-kit-positive CSCs were successfully isolated from the human right atrium and expanded and showed that they had a differentiation potential for endothelial rather than cardiomyogenic lineages, in vitro. Human CSC sheets were successfully transplanted into the swine chronic ischemic injury heart with minimal arrhythmogenicity and elicited global functional recovery in 8 weeks. CSC sheet transplantation concomitant with intramyocardial EPC injection showed enhanced global functional recovery compared with the CSC sheet-only therapy. Transplantation of the CSC

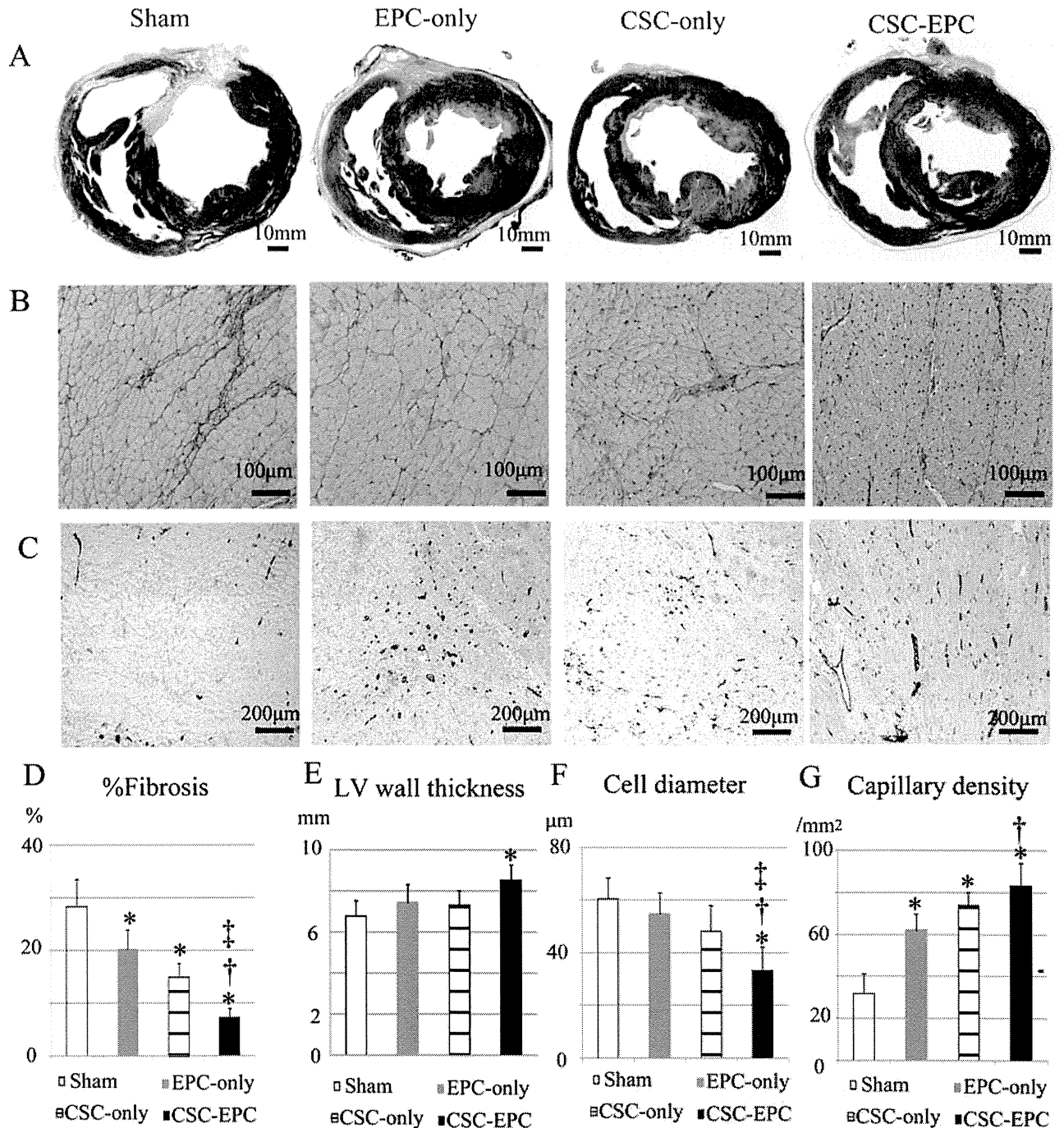


**Figure 6.** Histological assessment of interstitial fibrosis, capillary density, and myocyte hypertrophy 8 weeks after cell transplantation. (A) Representative Masson's trichrome staining in a section through the entire heart. (B) Representative periodic acid-Schiff staining of the remote zone. (C) Representative immunostaining for vWF in the peri-ischemic zone. (D) Quantification of fibrosis in each group ( $n=6$  each). (E) In the CSC-EPC group, the thickness of the LV wall was well preserved compared with the sham group ( $p<0.01$ , ANOVA). (F) Quantification of the cell diameter of myocytes ( $n=6$  each). (G) Quantification of capillary density at the peri-ischemic zone ( $n=6$  each). The number of vWF-positive capillaries of the CSC-EPC group was the greatest, followed by the CSC-only and EPC-only groups, and then the sham group ( $p<0.001$ , ANOVA). \* $p<0.05$  versus sham, † $p<0.05$  versus EPC-only, ‡ $p<0.05$  versus CSC-only. Abbreviations: vWF, von Willebrand factor; CSC, cardiac stem cell; EPC, endothelial progenitor cell; LV, left ventricular.

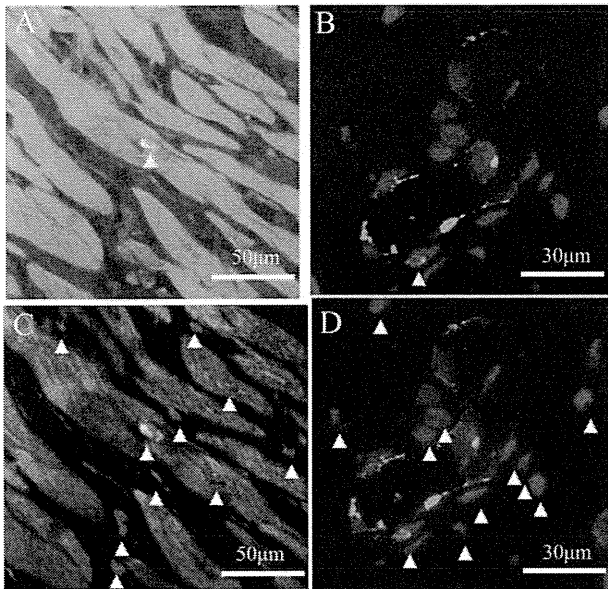


**Figure 7.** Phenotypic fate of transplanted CSCs and EPCs at 8 weeks posttreatment. (A, B) Representative immunostaining with human FISH (white/pink staining) and cTn-I (A; green) or vWF (B; green) in the CSC–EPC group. Small numbers of cardiomyocytes (A) and endothelial cells (B) with a human genome were present in the native myocardium. (C, D) Representative immunostaining with swine FISH and cTn-I (C) or vWF (D) in the CSC–EPC group. All the cardiomyocytes (C) and endothelial cells (D) that were positive for human genomic markers were also positive for porcine markers; thus, they had chimeric nuclei. Nuclear staining by DAPI is shown in blue. Yellow and white arrows indicate human and swine genomic markers, respectively. Abbreviations: CSC, cardiac stem cell; EPC, endothelial progenitor cell; FISH, fluorescence in situ hybridization; cTn-I, cardiac troponin I; vWF, von Willebrand factor.

sheet alone induced histological reverse LV remodeling, including attenuated interstitial fibrosis and increased vessel numbers, and concomitant EPC injection induced greater reverse LV remodeling effects than the CSC sheet-only therapy. Most of the transplanted CSCs were engrafted onto the surface over the ischemic area, while a small number migrated into the epicardium following the transplantation of the CSC sheet only. In contrast, concomitant EPC injection enhanced the migration of the transplanted CSCs into the myocardium, in association with local upregulations of SDF-1, VEGF, and IGF-1. While the CSCs of human origin in this study rarely differentiated into the cardiomyocytes in a porcine heart, transplantation of the CSCs induced functional and pathological recovery, suggesting that paracrine effects are the major therapeutic mechanisms in this study. Importantly, speckle-tracking echocardiography and histological data indicate that the CSCs and the EPCs produced different paracrine effects in the failing heart, suggesting synergic effects of these two cell types as shown in this study.

Clinical cell therapy has been reported to yield only modest functional recovery, as assessed by standard echocardiography (19,22). However, the latest echocardiographic methods, such as strain and contrast echocardiography, may better dissect layer-specific regional cardiac functions or myocardial perfusion, leading to a clearer understanding of the functional benefits of cell therapies. The adult mammalian heart is formed in three layers: contractile myocardium, inner endocardium, and outer epicardium. The layers differ in their contribution to cardiac performance and biological function (18). Myocardial infarction affects these myocardial layers to different extents, and ischemic change occurs in a wave-front pattern from the endocardium to the epicardium. In particular, the epicardium is thought to have a rich cardiac progenitor cell niche and to play an important role in cardiac repair (18,24,34). Of note, it has been shown that cell sheet implantation into the epicardium induces the expression of multiple cardioprotective factors in the heart and activates host epicardial cells crucial for cardiac repair through “crosstalk” between the implanted cell sheet and the native epicardium (20,33). This delivery method has also been demonstrated to maximize the retention and survival of the transplanted cells and to minimize the risks of cell delivery-related myocardial damage (23,27). Thus, we believed that the transplantation of CSCs by the cell sheet technique might have greater therapeutic effects in a swine chronic ischemic injury model than other delivery methods.

Our layer-specific analysis by strain echocardiography revealed that the CSC sheet transplantation induced significant functional improvement in myocardial function only in the ischemic epicardium. Consistent with this result, epicardial CSC sheet implantation induced neovascularization and reduced fibrosis in a paracrine manner in this area. We also observed the migration of transplanted CSCs into the native ischemic epicardium, which suggested that these functional and morphological benefits might be associated with the location of transplanted CSCs in the host myocardium. Previous reports demonstrated that the SDF-1–CXCR4 axis plays an important role in the migration of bone marrow and cardiac stem cells from the cell sheet to the infarct myocardium (17,28,29). Our data suggested that since migrated CSCs were located in the vicinity of SDF-1 in the host tissue, SDF-1 present in the ischemic tissue might promote the cell migration from the cell sheet to the native ischemic tissues. The strong expression of CXCR4 in the CSC sheet *in vitro* might support this scenario. In fact, the expressions of angiogenic growth factors, including SDF-1, in the chronic ischemic tissues were markedly diminished in the sham group, although these cytokines and adhesion molecules, which play important roles in cardiac repair after injury, are known to be abundant in

ischemic tissues at the acute stage of myocardial infarction (1). Thus, these microenvironmental factors in the host cardiac tissue might not greatly contribute to the therapeutic efficacy of the CSC sheet for the chronic ischemic injury model.

In contrast to CSC sheet transplantation, intramyocardial EPC injection significantly enhanced the improvement in myocardial function only in the ischemic and peri-ischemic endocardium, and not in the epicardium, in a paracrine manner. Urbich et al. reported that soluble factors released by EPCs promote the migration of cardiac-resident progenitor cells, using an *in vitro* migration assay (31). Thus, we considered that EPCs intramyocardially injected into the ischemic endocardium might promote the host tissue's expression of the angiogenic cytokine SDF-1, consequently enhancing the therapeutic efficacy of CSC sheet transplantation by improving the migration of the transplanted CSCs into the native ischemic myocardium.

The graft rate of transplanted EPCs by intramyocardial injection was lower than that of transplanted CSCs by the cell sheet technique. Transplanted CSCs were uniformly identified in the ischemic epicardium, whereas transplanted EPCs were densely located within the vascular wall of the ischemic and peri-ischemic endocardium. These different graft rates and patterns of transplanted cells might be related to the greater improvement in ESPVR and lower frequency (although not significant) of premature ventricular contraction seen in the animals receiving CSC sheet implantation alone compared with intramyocardial EPC injection alone, as previously described (20,26). One might think that EPCs could be mixed into the CSC sheet to enhance the CSCs' function; however, we have not been able to generate cell sheets from such mixed cultures. In addition, the injection of EPCs into the endocardial area might be important for attracting the migration of CSCs from the surface to the endocardial area.

In this study, contrast echocardiography dissected the improved myocardial perfusion that was seen 8 weeks after cell transplantation in all the cell therapy groups, but not the sham group. It has been shown that myocardial perfusion is impaired in chronic ischemic cardiomyopathy and that improved myocardial perfusion is associated with a suppression of LV remodeling (8). These findings indicate that the therapeutic efficacy in all the cell therapy groups might have been mainly attributable to the suppressive effects on LV remodeling. Consistent with this idea, multidetector CT showed that the increased rate of EDV between before and 8 weeks after treatment was less than 20% in all the cell therapy groups, but not in the sham group. On the other hand, invasive hemodynamic assessment using a conductance catheter also showed that CSC sheet implantation or the intramyocardial injection

of EPCs significantly improved measures of LV diastolic functions, such as  $\tau$  and EDP, compared with the sham operation. Previous reports demonstrated that the stiffness of the infarcted myocardium plays an important role in the postinfarction remodeling process (25). Thus, the different types of cell therapy we used may have had a softening effect on the scar tissue by increasing the cellularity, leading to a more pliable scar and less global cardiac remodeling.

In this study, *in vivo* CSC sheet implantation or concomitant EPC injection rarely induced the differentiation of transplanted CSCs into cardiomyogenic or vasculogenic lineages. Instead, all of the cardiac protein-expressing transplanted cells arose from fusion with existing myocytes or endothelial cells. Several lines of evidence support the idea that differentiation potential can be altered by differences in the severity of the pretreated infarct, as well as the timing of cell transplantation (20,21). In particular, Matsuura et al. reported that in viable ischemic tissues with existing cardiomyocytes, CSCs are likely to differentiate into myocytes or vascular cells via a cell fusion-dependent mechanism (20). Our layer-specific regional functional analysis by strain echocardiography identified residual viability in the ischemic area just before the cell therapies, and these conditions might have limited the differentiation potential of the CSC sheet *in vivo* and the ability of additional EPC injection to promote the differentiation of CSCs into the cardiomyogenic or vasculogenic lineages.

A potential limitation of this study is that the human c-kit-positive CSCs were obtained from a single donor. However, the isolation and culture methods for the primary c-kit-positive CSCs used in this study were previously established to yield CSCs of consistent functionality regardless of the donor (30). The findings of this study are therefore likely to be consistent with those obtained using CSCs from a different donor. In addition, although the swine were immunosuppressed by a previously reported regimen (15), xenogeneic cell transplantation might limit or exaggerate the therapeutic efficacy of the treatment. However, our analysis of layer-specific regional function clearly demonstrated the previously undescribed therapeutic benefit that additional EPC injection improves the CSC sheet therapy for the swine ischemic injury model.

In summary, CSC transplantation by the cell sheet technique prevented LV remodeling, through increased neovascularization and reduced fibrosis in a paracrine manner, and consequently improved the global LV function, and these effects were further enhanced by combination therapy with EPC injection. Our layer-specific strain analysis revealed that CSC sheet implantation improved regional wall motion in the epicardium, but not the endocardium. However, concomitant EPC transplantation significantly enhanced the therapeutic potential of CSC sheet

therapy in the endocardium. Concomitant EPC injection promoted migration of transplanted CSCs into the host myocardium, which might contribute to enhancement of functional recovery in the endocardium by the combination therapy. The combination of CSC sheet implantation and intramyocardial EPC injection may represent a promising strategy for ischemic cardiomyopathy.

**ACKNOWLEDGMENTS:** We thank Mr. Tsuyoshi Ishikawa for cell culturing and Mr. Shigeru Matsumi for excellent technical assistance for the surgery and care of the animals. This study was financially supported by a Grant-in-Aid of Scientific Research (08062134) from the Ministry of Health, Labour, and Welfare of Japan. Mr. Akima Harada is a full-time employee of CellSeed Inc., Japan. Mr. Tatsuya Shimizu and Mr. Teruo Okano are members of the scientific advisory board of CellSeed Inc., Japan. The authors declare no additional conflicts of interest.

## REFERENCES

- Abbott, J. D.; Huang, Y.; Liu, D.; Hickey, R.; Krause, D. S.; Giordano, F. J. Stromal cell-derived factor-1alpha plays a critical role in stem cell recruitment to the heart after myocardial infarction but is not sufficient to induce homing in the absence of injury. *Circulation* 110(21):3300–3305; 2004.
- Adamu, U.; Schmitz, F.; Becker, M.; Kelm, M.; Hoffmann, R. Advanced speckle tracking echocardiography allowing a three-myocardial layer-specific analysis of deformation parameters. *Eur. J. Echocardiogr.* 10(2):303–308; 2009.
- Becker, M.; Altiok, E.; Lente, C.; Otten, S.; Friedman, Z.; Adam, D.; Hoffmann, R.; Koos, R.; Krombach, G.; Marx, N. Layer-specific analysis of myocardial function for accurate prediction of reversible ischaemic dysfunction in intermediate viability defined by contrast-enhanced MRI. *Heart* 97(9):748–756; 2011.
- Becker, M.; Ocklenburg, C.; Altiok, E.; Futing, A.; Balzer, J.; Krombach, G.; Lysyansky, M.; Kuhl, H.; Krings, R.; Kelm, M.; Hoffmann, R. Impact of infarct transmural extent on layer-specific impairment of myocardial function: Amyocardial deformation imaging study. *Eur. Heart J.* 30(12):1467–1476; 2009.
- Bel, A.; Planat-Bernard, V.; Saito, A.; Bonnevie, L.; Bellamy, V.; Sabbah, L.; Bellabas, L.; Brinon, B.; Vanneaux, V.; Pradeau, P.; Peyrard, S.; Larghero, J.; Pouly, J.; Binder, P.; Garcia, S.; Shimizu, T.; Sawa, Y.; Okano, T.; Bruneval, P.; Desnos, M.; Hagege, A. A.; Casteilla, L.; Puceat, M.; Menasche, P. Composite cell sheets: A further step toward safe and effective myocardial regeneration by cardiac progenitors derived from embryonic stem cells. *Circulation* 122(11 Suppl):S118–123; 2010.
- Bolli, R.; Chugh, A. R.; D’Amario, D.; Loughran, J. H.; Stoddard, M. F.; Ikram, S.; Beache, G. M.; Wagner, S. G.; Leri, A.; Hosoda, T.; Sanada, F.; Elmore, J. B.; Goichberg, P.; Cappetta, D.; Solankhi, N. K.; Fahsah, I.; Rokosh, D. G.; Slaughter, M. S.; Kajstula, J.; Anversa, P. Cardiac stem cells in patients with ischaemic cardiomyopathy (SCPIO): Initial results of a randomised phase 1 trial. *Lancet* 378(9806):1847–1857; 2011.
- Dib, N.; Khawaja, H.; Varner, S.; McCarthy, M.; Campbell, A. Cell therapy for cardiovascular disease: A comparison of methods of delivery. *J. Cardiovasc. Transl. Res.* 4(2):177–181; 2011.
- Galiuto, L.; Garramone, B.; Scara, A.; Rebuzzi, A. G.; Crea, F.; La Torre, G.; Funaro, S.; Madonna, M.; Fedele, F.; Agati, L. The extent of microvascular damage during myocardial contrast echocardiography is superior to other known indexes of post-infarct reperfusion in predicting left ventricular remodeling: Results of the multicenter AMICI study. *J. Am. Coll. Cardiol.* 51(5):552–559; 2008.
- Hosoda, T.; Zheng, H.; Cabral-da-Silva, M.; Sanada, F.; Ide-Iwata, N.; Ogorek, B.; Ferreira-Martins, J.; Arranto, C.; D’Amario, D.; del Monte, F.; Urbanek, K.; D’Alessandro, D. A.; Michler, R. E.; Anversa, P.; Rota, M.; Kajstula, J.; Leri, A. Human cardiac stem cell differentiation is regulated by a mircrine mechanism. *Circulation* 123(12):1287–1296; 2011.
- Imanishi, Y.; Miyagawa, S.; Meaeda, N.; Fukushima, S.; Kitagawa-Sakakida, S.; Daimon, T.; Hirata, A.; Shimizu, T.; Okano, T.; Shimomura, I.; Sawa, Y. Induced adipocyte cell-sheet ameliorates cardiac dysfunction in a mouse myocardial infarction model: A novel drug delivery system for heart failure. *Circulation* 124(suppl 1):S10–S17; 2011.
- Iwasaki, H.; Kawamoto, A.; Ishikawa, M.; Oyamada, A.; Nakamori, S.; Nishimura, H.; Sadamoto, K.; Horii, M.; Matsumoto, T.; Murasawa, S.; Shibata, T.; Suehiro, S.; Asahara, T. Dose-dependent contribution of CD34-positive cell transplantation to concurrent vasculogenesis and cardiomyogenesis for functional regenerative recovery after myocardial infarction. *Circulation* 113(10):1311–1325; 2006.
- Kawaguchi, N.; Smith, A. J.; Waring, C. D.; Hasan, M. K.; Miyamoto, S.; Matsuoka, R.; Ellison, G. M. c-kit<sup>pos</sup> GATA-4 high rat cardiac stem cells foster adult cardiomyocyte survival through IGF-1 paracrine signalling. *PLoS One* 5(12):e14297; 2010.
- Kawamoto, A.; Iwasaki, H.; Kusano, K.; Murayama, T.; Oyamada, A.; Silver, M.; Hulbert, C.; Gavin, M.; Hanley, A.; Ma, H.; Kearney, M.; Zak, V.; Asahara, T.; Losordo, D. W. CD34-positive cells exhibit increased potency and safety for therapeutic neovascularization after myocardial infarction compared with total mononuclear cells. *Circulation* 114(20):2163–2169; 2006.
- Kempny, A.; Diller, G. P.; Kaleschke, G.; Orwat, S.; Funke, A.; Radke, R.; Schmidt, R.; Kerckhoff, G.; Ghezelbash, F.; Rukosujew, A.; Reinecke, H.; Scheld, H. H.; Baumgartner, H. Longitudinal left ventricular 2D strain is superior to ejection fraction in predicting myocardial recovery and symptomatic improvement after aortic valve implantation. *Int. J. Cardiol.* 167(5):2239–2243; 2013.
- Kim, B. O.; Tian, H.; Prasongsukarn, K.; Wu, J.; Angoulvant, D.; Wnendt, S.; Muhs, A.; Spitkovsky, D.; Li, R. K. Cell transplantation improves ventricular function after a myocardial infarction: A preclinical study of human unrestricted somatic stem cells in a porcine model. *Circulation* 112(9 Suppl):I96–104; 2005.
- Kobayashi, H.; Shimizu, T.; Yamato, M.; Tono, K.; Masuda, H.; Asahara, T.; Kasanuki, H.; Okano, T. Fibroblast sheets co-cultured with endothelial progenitor cells improve cardiac function of infarcted hearts. *J. Artif. Organs* 11(3):141–147; 2008.
- Li, N.; Lu, X.; Zhao, X.; Xiang, F. L.; Xenocostas, A.; Karmazyn, M.; Feng, Q. Endothelial nitric oxide synthase promotes bone marrow stromal cell migration to the ischemic myocardium via upregulation of stromal cell-derived factor-1alpha. *Stem Cells* 27(4):961–970; 2009.

18. Limana, F.; Zacheo, A.; Mocini, D.; Mangoni, A.; Borsellino, G.; Diamantini, A.; De Mori, R.; Battistini, L.; Vigna, E.; Santini, M.; Loiaconi, V.; Pompilio, G.; Germani, A.; Capogrossi, M. C. Identification of myocardial and vascular precursor cells in human and mouse epicardium. *Circ. Res.* 101(12):1255–1265; 2007.
19. Makkar, R. R.; Smith, R. R.; Cheng, K.; Malliaras, K.; Thomson, L. E.; Berman, D.; Czer, L. S.; Marban, L.; Mendizabal, A.; Johnston, P. V.; Russell, S. D.; Schuleri, K. H.; Lardo, A. C.; Gerstenblith, G.; Marban, E. Intracoronary cardiosphere-derived cells for heart regeneration after myocardial infarction (CADUCEUS): A prospective, randomised phase 1 trial. *Lancet* 379(9819):895–904; 2012.
20. Matsuura, K.; Honda, A.; Nagai, T.; Fukushima, N.; Iwanaga, K.; Tokunaga, M.; Shimizu, T.; Okano, T.; Kasanuki, H.; Hagiwara, N.; Komuro, I. Transplantation of cardiac progenitor cells ameliorates cardiac dysfunction after myocardial infarction in mice. *J. Clin. Invest.* 119:2204–2217; 2009.
21. Matsuura, K.; Wada, H.; Nagai, T.; Iijima, Y.; Minamino, T.; Sano, M.; Akazawa, H.; Molkenstein, J. D.; Kasanuki, H.; Komuro, I. Cardiomyocytes fuse with surrounding noncardiomyocytes and reenter the cell cycle. *J. Cell Biol.* 167(2):351–363; 2004.
22. Meyer, G. P.; Wollert, K. C.; Lotz, J.; Steffens, J.; Lippolt, P.; Fichtner, S.; Hecker, H.; Schaefer, A.; Arseniev, L.; Hertenstein, B.; Ganser, A.; Drexler, H. Intracoronary bone marrow cell transfer after myocardial infarction: Eighteen months' follow-up data from the randomized, controlled BOOST (Bone marrow transfer to enhance ST-elevation infarct regeneration) trial. *Circulation* 113(10):1287–1294; 2006.
23. Miyagawa, S.; Saito, A.; Sakaguchi, T.; Yoshikawa, Y.; Yamauchi, T.; Imanishi, Y.; Kawaguchi, N.; Teramoto, N.; Matsuura, N.; Iida, H.; Shimizu, T.; Okano, T.; Sawa, Y. Impaired myocardium regeneration with skeletal cell sheets—A preclinical trial for tissue-engineered regeneration therapy. *Transplantation* 90(4):364–372; 2010.
24. Russell, J. L.; Goetsch, S. C.; Gaiano, N. R.; Hill, J. A.; Olson, E. N.; Schneider, J. W. A dynamic notch injury response activates epicardium and contributes to fibrosis repair. *Circ. Res.* 108(1):51–59; 2011.
25. Schneider, C.; Jaquet, K.; Geidel, S.; Rau, T.; Malisius, R.; Boczor, S.; Zienkiewicz, T.; Kuck, K. H.; Krause, K. Transplantation of bone marrow-derived stem cells improves myocardial diastolic function: Strain rate imaging in a model of hibernating myocardium. *J. Am. Soc. Echocardiogr.* 22(10):1180–1189; 2009.
26. Sekine, H.; Shimizu, T.; Dobashi, I.; Matsuura, K.; Hagiwara, N.; Takahashi, M.; Kobayashi, E.; Yamato, M.; Okano, T. Cardiac cell sheet transplantation improves damaged heart function via superior cell survival in comparison with dissociated cell injection. *Tissue Eng. Part A* 17(23–24):2973–2980; 2011.
27. Shimizu, T.; Sekine, H.; Yamato, M.; Okano, T. Cell sheet-based myocardial tissue engineering: New hope for damaged heart rescue. *Curr. Pharm. Design* 15(24):2807–2814; 2009.
28. Son, B. R.; Marquez-Curtis, L. A.; Kucia, M.; Wysoczynski, M.; Turner, A. R.; Ratajczak, J.; Ratajczak, M. Z.; Janowska-Wieczorek, A. Migration of bone marrow and cord blood mesenchymal stem cells in vitro is regulated by stromal-derived factor-1-CXCR4 and hepatocyte growth factor-c-met axes and involves matrix metalloproteinases. *Stem Cells* 24(5):1254–1264; 2006.
29. Tang, J. M.; Wang, J. N.; Zhang, L.; Zheng, F.; Yang, J. Y.; Kong, X.; Guo, L. Y.; Chen, L.; Huang, Y. Z.; Wan, Y.; Chen, S. Y. VEGF/SDF-1 promotes cardiac stem cell mobilization and myocardial repair in the infarcted heart. *Cardiovasc. Res.* 91(3):402–411; 2011.
30. Tang, X. L.; Rokosh, G.; Sanganalmath, S. K.; Yuan, F.; Sato, H.; Mu, J.; Dai, S.; Li, C.; Chen, N.; Peng, Y.; Dawn, B.; Hunt, G.; Leri, A.; Kajstura, J.; Tiwari, S.; Shirk, G.; Anversa, P.; Bolli, R. Intracoronary administration of cardiac progenitor cells alleviates left ventricular dysfunction in rats with a 30-day-old infarction. *Circulation* 121(2):293–305; 2010.
31. Urbich, C.; Aicher, A.; Heeschen, C.; Dernbach, E.; Hofmann, W. K.; Zeiher, A. M.; Dimmeler, S. Soluble factors released by endothelial progenitor cells promote migration of endothelial cells and cardiac resident progenitor cells. *J. Mol. Cell. Cardiol.* 39(5):733–742; 2005.
32. Wollert, K. C.; Meyer, G. P.; Lotz, J.; Ringes-Lichtenberg, S.; Lippolt, P.; Breidenbach, C.; Fichtner, S.; Korte, T.; Hornig, B.; Messinger, D.; Arseniev, L.; Hertenstein, B.; Ganser, A.; Drexler, H. Intracoronary autologous bone-marrow cell transfer after myocardial infarction: The BOOST randomised controlled clinical trial. *Lancet* 364(9429):141–148; 2004.
33. Zakharova, L.; Mastroeni, D.; Mutlu, N.; Molina, M.; Goldman, S.; Diethrich, E.; Gaballa, M. A. Transplantation of cardiac progenitor cell sheet onto infarcted heart promotes cardiogenesis and improves function. *Cardiovasc. Res.* 87(1):40–49; 2010.
34. Zhou, B.; Ma, Q.; Rajagopal, S.; Wu, S. M.; Domian, I.; Rivera-Feliciano, J.; Jiang, D.; von Gise, A.; Ikeda, S.; Chien, K. R.; Pu, W. T. Epicardial progenitors contribute to the cardiomyocyte lineage in the developing heart. *Nature* 454(7200):109–113; 2008.